Research Square

Preprints are preliminary reports that have not undergone peer review.
They should not be considered conclusive, used to inform clinical practice,
or referenced by the media as validated information.

Underlying Mechanism of Prohexadione Calcium-Mediated Alleviation of Salt Stress-Induced Damage via Modulation of Leaf Lipid Metabolism, Chloroplast Structure and Photosynthetic Performance in Rice Seedlings

Yuqiang Qiu
Guangdong Ocean University
Naijie Feng
fengj@gdou.cn
Guangdong Ocean University
Xiao Wang
Guangdong Ocean University
Ziming Chen
Guangdong Ocean University
Hanxing Ning
Guangdong Ocean University
Yue Zhao
Guangdong Ocean University
Guoyang Shao
Guangdong Ocean University
Hongjie Chen
Guangdong Ocean University

Research Article

Keywords: Salt、Rice、Pro-Ca、Lipid Metabolism

Posted Date: November 5th, 2026

DOI: https://doi.org/10.21203/rs.3.rs-11291810/v1

License: This work is licensed under a Creative Commons Attribution 4.0 International License.
Read Full License

Additional Declarations: No competing interests reported.

Underlying Mechanism of Prohexadione Calcium-Mediated Alleviation of Salt Stress-Induced Damage via Modulation of Leaf Lipid Metabolism, Chloroplast Structure and Photosynthetic Performance in Rice Seedlings

Yuqiang Qiu[1+]、Naijie Feng[1、2、3*]、Xiao Wang[1]、Ziming Cheng[1]、Hanxing Ning[1]、Yue Zhao[1]、Guoyang Shao[1]、Hongjie Cheng[1]

[+]Yuqiang Qiu is the first author, responsible for manuscript writing, experiment execution and data analysis.

*Correspondence:NaiJie Feng fengj@gdou.cn

Full list of author information is available at the end of the article

Abstract

Rice (*Oryza sativa* L.) is a staple food crop in China, where salt stress poses a severe constraint on rice growth and development. Prohexadione calcium (Pro-Ca) has been recognized as an effective regulator in mitigating salt stress damage in rice. In this pot experiment, two rice cultivars—the salt-sensitive Huanghuazhan (HHZ) and the salt-tolerant Guanghong No. 3 (GH3)—were used as plant materials. Foliar application of Pro-Ca was conducted at the three-leaf stage, followed by NaCl treatment at the four-leaf stage. Three treatments were established: (1) 0 mM NaCl + 0 mg·L^{-1} Pro-Ca (control, CK); (2) 70 mM NaCl + 0 mg·L^{-1} Pro-Ca (salt stress, S); (3) 70 mM NaCl + 100 mg·L^{-1} Pro-Ca (salt stress + Pro-Ca, SP). On day 11 after NaCl exposure, untargeted lipidomics profiling was performed. Chloroplast ultrastructure was observed via transmission electron microscopy on day 21, and photosynthetic gas exchange parameters 【net photosynthetic rate（Pn）, intercellular CO_2 concentration （Ci）, stomatal conductance（Gs）, transpiration rate （Tr) and photosynthetic pigment concentrations (chlorophyll a, chlorophyll b, carotenoids, total chlorophyll)】 were quantified on day 31 after salt treatment. The underlying mechanism by which Pro-Ca alleviates salt stress-induced damage was elucidated based on the sequential alterations in lipid metabolites, chloroplast ultrastructure, and photosynthetic function.Our results revealed that at the lipid metabolic level, GH3 exhibited a much stronger lipidomic response to

salt stress than HHZ, with 283 and 35 differentially accumulated lipids identified, respectively. GH3 showed coordinated remodeling across multiple lipid classes, including dysregulated galactolipids (up-regulated DGDG and partially down-regulated MGDG), reduced phospholipids, and accumulated glycerolipids. By contrast, the lipid response in HHZ was dominated solely by the passive accumulation of glycerolipids (TG and DG). At the chloroplast ultrastructural level, HHZ chloroplasts displayed more severe disintegration of thylakoid lamellae and greater accumulation of osmiophilic plastoglobules, whereas GH3 chloroplasts retained better overall morphology and intact grana architecture. With respect to photosynthetic performance, HHZ was characterized by a marked decline in stomatal parameters accompanied by only a minor reduction in photosynthetic pigment contents, while GH3 exhibited substantial degradation of photosynthetic pigments.Our findings demonstrated that foliar application of Pro-Ca conferred stepwise alleviation of salt stress damage via the regulation of leaf lipid homeostasis. Specifically, Pro-Ca first prioritized the remodeling of leaf lipid profiles and restored membrane lipid composition by modulating glycerolipid metabolism and phospholipid biosynthesis pathways. This lipidomic remodeling subsequently facilitated the restoration of ordered thylakoid grana stacking, reduced the accumulation of osmiophilic plastoglobules, and preserved chloroplast structural integrity. Ultimately, these improvements translated into elevated photosynthetic gas exchange parameters and photosynthetic pigment contents, thereby mitigating salt-induced photosynthetic damage.Notably, the alleviatory effects of Pro-Ca exhibited pronounced genotype specificity. In HHZ, Pro-Ca predominantly targeted the clearance of excess accumulated glycerolipids, leading to a comprehensive recovery of all eight measured photosynthetic traits. In GH3, by contrast, Pro-Ca exerted synergistic protective effects by activating multiple biosynthetic pathways including galactolipid and phospholipid metabolism, resulting in a substantial increase in net photosynthetic rate (Pn).Pathway enrichment analysis indicated that glycerolipid metabolism was the only significantly enriched KEGG pathway in response to Pro-Ca treatment in HHZ ($Q < 0.05$). The phospholipid biosynthesis pathway showed a strong enrichment trend in the SMPDB database across both cultivars.Collectively, this study elucidates the mechanism by which Pro-Ca mitigates salt-induced photosynthetic damage in rice through modulating leaf lipid homeostasis and maintaining chloroplast structural integrity. The marked genotype-specific regulatory patterns identified herein provide a theoretical basis for the stress-resistant cultivation of rice in saline-alkali soils.

Key words: Salt、Rice、Pro-Ca、Lipid Metabolism

1. Introduction

Soil salinity represents one of the most pervasive abiotic stressors limiting agricultural productivity worldwide, and imposes severe constraints on crop yield formation and quality development(Fahad et al., 2019; Landi et al., 2017).Soil salinization imposes profound constraints on plant growth and development, and perturbs a wide spectrum of physiological and biochemical processes, ultimately leading to impaired crop productivity(C. Liu et al., 2022; Wang et al., 2015).Over recent decades, the global extent of saline-alkali soils has been expanding continuously, driven by multiple factors including global climate warming, unsustainable irrigation practices, and imbalanced fertilization management(Ye et al., 2021).

Rice (*Oryza sativa* L.) is generally classified as a salt-sensitive glycophyte(Ahmadi et al., 2011), yet it represents a promising pioneer crop for soil amelioration in coastal tidal flat ecosystems. Globally, approximately 30% of rice-cultivated areas are subjected to varying degrees of salt stress(Prasad, 2000).Exploiting coastal tidal flats for rice production can directly expand arable rice acreage, which holds great practical importance for mitigating cultivated land scarcity and safeguarding regional food security.Salt stress impairs water and nutrient uptake capacity in rice(Zhang, 2010), triggers ion cytotoxicity and oxidative damage(Yadav, 2011), and consequently compromises the integrity of cellular membrane systems(Yang, 2018; Zhan et al., 2019).Furthermore, excessive salt exposure disrupts chloroplast thylakoid membrane architecture(Rachana Ouk, 2024), uppresses chlorophyll biosynthesis and reduces chlorophyll pools, and restricts dry matter assimilation in plants, all of which collectively severely retard rice growth and development.

Photosynthesis serves as the central physiological process underlying dry matter assimilation and yield formation in rice. Under saline conditions, rice leaves exhibit repressed chlorophyll biosynthesis and accelerated pigment degradation, leading to a marked reduction in photosynthetic pigment pools, coupled with diminished PSⅡ photochemical efficiency, which collectively constrains overall photosynthetic capacity(Rongjun Zhang, 2023; Yamane, 2008).At the subcellular structural level, chloroplasts function as the primary site of photosynthesis, and their morphological integrity and ultrastructural organization constitute the structural foundation for efficient photosynthetic performance. Evidence from transmission electron microscopy and three-dimensional ultrastructural reconstruction has demonstrated that salt stress induces profound structural alterations in chloroplasts of rice mesophyll cells.

Normally ellipsoidal chloroplasts aligned along the cell wall become shrunken and distorted; the chloroplast envelope suffers partial disruption or complete disintegration; the thylakoid membrane system becomes swollen and disorganized with collapsed grana stacking; and massive osmiophilic plastoglobules accumulate concurrently(Jiang et al., 2020; Oi et al., 2020; Rachana Ouk, 2024).Furthermore, disrupted ion homeostasis under salt stress exacerbates oxidative damage and functional deterioration of photosynthetic apparatus(Xie et al., 2025).Importantly, the structural integrity and functional competence of chloroplast thylakoid membranes are strongly dependent on their membrane lipid profiles, positioning membrane lipids as a critical mechanistic link between chloroplast ultrastructure and photosynthetic function.

Biological membranes act as the first line of defense against environmental stresses in plants. Preserving membrane stability and integrity under saline conditions is critical for mitigating salt-induced cytotoxicity, as membrane integrity is a prerequisite for sustaining cellular homeostasis(Lv, 2021; Mansour, 2013).Plant membrane lipids are classified into three major classes: sphingolipids, sterols, and glycerolipids(Borrell, 2016).Membrane glycerolipids are defined by a glycerol backbone esterified with either a phosphate head group (phospholipids) or a carbohydrate moiety (glycolipids)(Guo et al., 2019).The phospholipid fraction is primarily composed of phosphatidylcholine (PC), phosphatidylethanolamine (PE), phosphatidic acid (PA), phosphatidylinositol (PI), and phosphatidylserine (PS). In chloroplasts, the predominant glycolipids are monogalactosyldiacylglycerol (MGDG), digalactosyldiacylglycerol (DGDG), and sulfoquinovosyldiacylglycerol (SQDG), whereas phosphatidylglycerol (PG) represents the most abundant phospholipid species in thylakoid membranes(Kalisch et al., 2016).Collectively, MGDG and DGDG constitute the bulk of thylakoid membrane lipids, accounting for approximately 50% and 25% of the total thylakoid lipid pool, respectively(Block, 1983).Compelling evidence indicates that a reduction in MGDG content is a conserved hallmark of plant responses to a range of osmotic stresses, including salinity, drought, and low temperature. Remodeling of membrane lipid composition therefore represents a key adaptive strategy for plants to maintain membrane fluidity and counteract oxidative damage under stress conditions(Gigon, 2004; Welti et al., 2002).Among phospholipid species, the PC/PE ratio is closely linked to plant salt tolerance: plants with a higher PC/PE ratio in biological membranes generally exhibit superior salt tolerance relative to those with lower ratios. Phosphatidylinositol bisphosphate (PIP_2), another well-characterized

signaling phospholipid, also participates in plant salt stress responses(Li et al., 2016; Omoto, 2016).

Among exogenous strategies for mitigating salt stress damage, the application of plant growth regulators has garnered considerable research attention(Z. Liu et al., 2022).Prohexadione-calcium (Pro-Ca) is a well-characterized plant growth regulator that acts as a competitive inhibitor of key enzymes in the gibberellin biosynthetic pathway, thereby reducing bioactive gibberellin levels and modulating endogenous hormone homeostasis in plants(Rademacher, 2015).Accumulating evidence demonstrates that exogenous application of Pro-Ca at appropriate concentrations confers salt tolerance in rice by boosting osmolyte accumulation, enhancing antioxidant enzyme activities, and ameliorating ion cytotoxicity(Zhang R, 2023).In soybean seedlings, foliar application of Pro-Ca has been reported to suppress chlorophyll degradation, attenuate thylakoid structural disruption, and improve photosynthetic performance including net photosynthetic rate, PSⅡ potential activity (Fv/Fo), and maximum photochemical quantum yield of PSⅡ (Fv/Fm)(Feng et al., 2021).Nevertheless, existing studies on Pro-Ca-mediated salt tolerance in rice have largely focused on physiological phenotypes and transcriptional regulation. The regulatory mechanism of Pro-Ca at the lipid metabolic level remains largely unexplored in rice. Furthermore, the inter-cultivar differences in lipid remodeling patterns under salt stress and the genotypic specificity of Pro-Ca regulation between salt-sensitive and salt-tolerant rice cultivars are still poorly understood.

Huanghuazhan (HHZ) and Guanghong No. 3 (GH3) are widely grown elite rice cultivars in the South China rice production area, and their contrasting salt tolerance makes them representative and well-suited experimental materials for investigating rice salt stress responses and exogenous regulatory mechanisms. In this study, using seedling-stage plants of the two rice cultivars as materials, we integrated photosynthetic physiological assays, chloroplast ultrastructural observation, and untargeted lipidomics profiling to systematically dissect the differential responses of photosynthetic performance, chloroplast architecture, and lipid metabolism between the two cultivars under salt stress. We further elucidated the underlying mechanism by which Pro-Ca preserves chloroplast structural integrity and mitigates photosynthetic damage via the regulation of lipid homeostasis. Collectively, this study provides theoretical insights and experimental evidence for stress-resistant rice cultivation in saline-alkali soils and the rational application of plant growth regulators.

2、Materials and Methods

2.1Plant Materials and Growth Conditions

A pot experiment was conducted using two rice cultivars: the salt-tolerant Guanghong No. 3 (GH3) and the salt-sensitive Huanghuazhan (HHZ). Among them, the Guanghong No.3 seeds come from the Guangdong Academy of Agricultural Sciences, and the Huahuazhan seeds come from Shenzhen Jingulong Seed Co., Ltd.Three treatments were established for each cultivar: (1) control (CK): 0 mM NaCl + 0 mg·L^{-1} Pro-Ca; (2) salt stress (S): 70 mM NaCl + 0 mg·L^{-1} Pro-Ca; (3) salt stress + Pro-Ca (SP): 70 mM NaCl + 100 mg·L^{-1} Pro-Ca. The treatment groups were abbreviated as HCK, HS and HSP for HHZ, and GCK, GS and GSP for GH3, respectively.Rice seeds were surface-sterilized with 3% (v/v) sodium hypochlorite solution for 15 min and rinsed thoroughly with distilled water. The seeds were then soaked in distilled water at 30℃ for 24 h, rinsed five times with distilled water, spread uniformly in plastic Petri dishes, and pre-germinated in a constant-temperature incubator at 30℃ for 24 h. Uniformly germinated seeds were selected and sown in plastic nursery trays for seedling cultivation. Foliar application of Pro-Ca at a concentration of 100 mg·L^{-1} was performed at the three-leaf stage. At the four-leaf stage, seedlings with consistent growth vigor were transplanted into green plastic buckets (27 cm in diameter) filled with 8 kg of lateritic red soil. Following a 3-day acclimation period, salt stress was imposed by irrigating with 70 mM NaCl solution, whereas control plants received an equal volume of distilled water. Plant samples were collected at 11, 21, and 31 days after the initiation of salt stress for subsequent analyses.

2.2Lipidomics Profiling Analysis

Leaf samples were harvested at 11 days after the initiation of salt stress, immediately snap-frozen in liquid nitrogen, and stored at −80 ℃ until processing. Lipid extraction and mass spectrometry-based lipid profiling were conducted by Guangzhou Zhi'ao Biotechnology Co., Ltd. (Guangzhou, China).

2.2.1 Sample Pretreatment and Lipid Extraction

Frozen leaf samples were homogenized and aliquoted to an appropriate amount. After adding 200 μL of deionized water, the mixture was vortexed thoroughly. Subsequently, 800 μL of methyl tert-butyl ether (MTBE) was added, followed by vortex mixing. Then 240 μL of pre-

chilled methanol was added and the mixture was vortexed again. Ultrasonication was performed for 20 min in an ice-cold water bath, followed by incubation at room temperature for 30 min to allow phase separation. The mixture was centrifuged at 14,000 × g for 15 min at 10 ℃. The upper organic phase was collected and evaporated to dryness under a gentle nitrogen stream. Prior to mass spectrometric analysis, the dried lipid residues were reconstituted in 200 μL of 90% (v/v) isopropanol/acetonitrile solution and vortexed thoroughly. A 90 μL aliquot of the reconstituted solution was centrifuged again at 14,000 × g for 15 min at 10 ℃, and the resulting supernatant was used for injection analysis.

2.2.2 Chromatographic and Mass Spectrometric Conditions

Chromatographic separation was carried out on a Nexera LC-30A ultra-high performance liquid chromatography (UHPLC) system (Shimadzu, Kyoto, Japan). To minimize instrumental signal drift and batch variation, all samples were analyzed sequentially in a randomized order. Mass spectrometric detection was performed on a Q Exactive hybrid quadrupole-Orbitrap mass spectrometer (Thermo Fisher Scientific, Waltham, MA, USA) coupled online to the UHPLC system.

2.2.3 Lipid Identification

Raw mass spectrometric data (.raw format) were processed for lipid annotation using LipidSearch software (Thermo Fisher Scientific, Waltham, MA, USA). Preprocessing steps including peak alignment, peak picking, and peak extraction were performed on both endogenous lipid species and internal standard lipids, generating a data matrix containing mass-to-charge ratio (m/z), retention time (RT), and peak intensity for each detected lipid feature. To enable quantitative comparison across samples with different abundance ranges, intra-class normalization of peak intensities was applied within each lipid category. Final lipid identification was confirmed via tandem mass spectrometry (MS/MS, secondary identification) against the LipidSearch in-built database.

2.3 Transmission Electron Microscopy for Chloroplast Ultrastructure

Leaf samples were collected at 21 days after salt stress for chloroplast ultrastructure analysis. Fresh leaf segments were cut into 1 mm × 2 mm × 3 mm rectangular strips with a sharp razor blade, and immediately fixed in 2.5% (v/v) glutaraldehyde in 0.1 M

phosphate-buffered saline (PBS, pH 7.4). Vacuum infiltration was performed to ensure complete penetration of the fixative into leaf tissues, and samples were stored at 4 ℃ in the dark.

For post-fixation, samples were incubated in 0.1 M phosphate buffer (PB, pH 7.4) containing 1% (w/v) osmium tetroxide for 7 h at room temperature under dark conditions. Following dehydration through a graded series of anhydrous ethanol and clearance with acetone, samples were embedded in Epon 812 epoxy resin. Ultrathin sections (70–90 nm) were prepared using an ultramicrotome, stained with 2.6% (w/v) lead citrate solution for 8 min, and examined under an HT7800 transmission electron microscope (Hitachi, Tokyo, Japan)(Du et al., 2024).

2.4 Measurement of Photosynthetic Gas Exchange Parameters

At 31 days after salt stress in rice, the net photosynthetic rate (Pn), intercellular CO_2 concentration (Ci), transpiration rate (Tr) and stomatal conductance (Gs) were measured from 9:00 to 11:00 under sufficient sunlight using a LI-6800 portable photosynthesis measurement system (LI-6800, LI-COR, Lincoln, NE, USA), with three replicates per treatment(Sales et al., 2022).The conditions inside the leaf chamber were set as follows: photosynthetically active radiation (PAR) of 1000 $\mu mol \cdot m^{-2} \cdot s^{-1}$, CO_2 concentration of 400 $\mu mol \cdot mol^{-1}$, leaf temperature of 30.0 ℃, relative air humidity of 70%–80%, and air flow rate of 500 $\mu mol \cdot s^{-1}$.

2.5 Measurement of Photosynthetic Pigments

Simultaneously with the measurement of photosynthetic gas exchange parameters, chlorophyll a (Chl a), chlorophyll b (Chl b), carotenoids (Car) and total chlorophyll (Chl a + b) were determined using the method proposed by Kolomeichuk(Kolomeichuk et al., 2020).Fresh leaf samples (0.1 g) were soaked in 10 mL of 95% ethanol for 24 h in the dark. The concentrations of Chl a, Chl b and Car were determined by spectrophotometry at wavelengths of 665, 649 and 470 nm, respectively.

$$\text{Chlorophyll a (Chl a)} = 13.95D_{665} - 6.88D_{649}$$

$$\text{Chlorophyll b (Chl b)} = 24.96D_{649} - 7.32D_{665}$$

$$\text{Total chlorophyll content} = \text{Chl a} + \text{Chl b}$$

$$\text{Carotenoids (Car)} = (1000\ D_{470} - 2.05\ \text{Chl a} - 111.48\ \text{Chl b})/245$$

2.6 Statistical Analysis

All values are expressed as mean ± standard deviation (SD). Statistical analyses were carried out using IBM SPSS Statistics 27 (IBM Corp., Armonk, NY, USA). One-way analysis of variance (ANOVA) was applied to evaluate the effects of different treatments, followed by Duncan's multiple range test for post hoc pairwise comparisons. A probability level of $P < 0.05$ was defined as statistically significant. Data collation and preliminary processing were performed in Microsoft Excel 2026, and all graphical visualizations were generated using Origin Pro 2025 (OriginLab Corp., Northampton, MA, USA).

三、Results

3.1 Effects of Pro-Ca on Photosynthetic Pigment Contents and Gas Exchange Parameters in Rice Seedlings Under Salt Stress

Salt stress significantly impaired photosynthetic gas exchange capacity and reduced photosynthetic pigment accumulation in rice seedlings. Both cultivars exhibited consistent reductions in net photosynthetic rate (Pn), intercellular CO_2 concentration (Ci), stomatal conductance (Gs), transpiration rate (Tr), and all measured photosynthetic pigment contents under salt stress conditions (Figure 3A–H). Foliar application of Pro-Ca effectively mitigated these salt-induced suppressions, leading to a general recovery of photosynthetic pigments and gas exchange parameters in both cultivars.

Compared with the control (CK), salt stress (S) significantly reduced Pn, Ci, Gs, Tr, chlorophyll a, chlorophyll b, total chlorophyll, and carotenoid contents in the salt-sensitive cultivar HHZ by 52.37%, 6.06%, 47.71%, 50.80%, 4.31%, 10.72%, 8.71%, and 9.78%, respectively. For the salt-tolerant cultivar GH3, the corresponding reductions under salt stress were 56.42%, 7.20%, 18.95%, 17.26%, 20.55%, 20.22%, 16.02%, and 24.90%, respectively.

Compared with the S treatment, Pro-Ca application (SP) significantly elevated Pn, Ci, Gs, Tr, chlorophyll a, chlorophyll b, total chlorophyll, and carotenoid contents in HHZ by 14.28%, 1.74%, 19.32%, 29.35%, 19.36%, 17.13%, 15.14%, and 11.25%, respectively. In GH3, Pro-Ca treatment significantly increased Pn, Ci, Gs, chlorophyll a, chlorophyll b, total chlorophyll, and carotenoid contents by 44.52%, 6.56%, 1.30%, 3.06%, 0.45%, 2.06%, and 10.20%, respectively, whereas transpiration rate (Tr) showed a 6.47% decrease relative to the salt-stressed group.

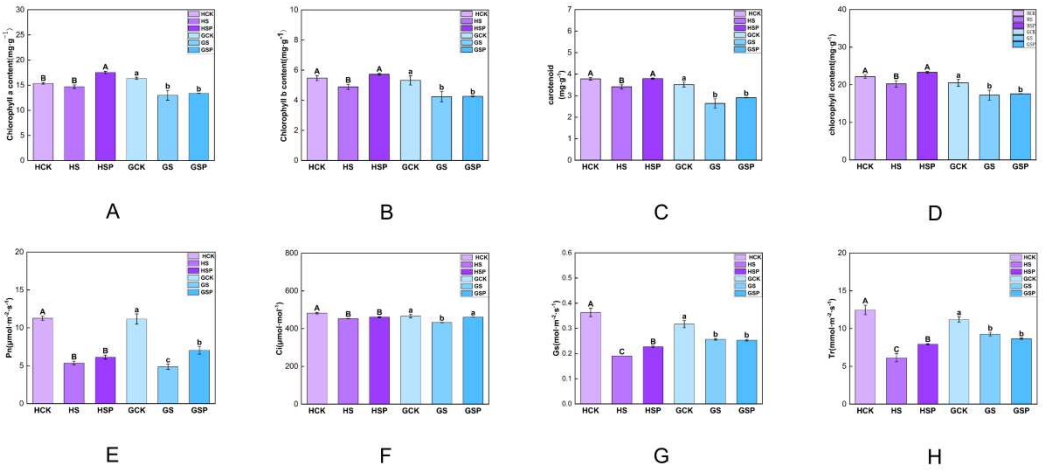


Figure 1. Effects of exogenous Pro-Ca application on photosynthetic pigment contents and gas exchange parameters in rice seedlings under salt stress. (A) Chlorophyll a content; (B) Chlorophyll b content; (C) Carotenoid content; (D) Total chlorophyll content; (E) Net photosynthetic rate (Pn); (F) Intercellular CO_2 concentration (Ci); (G) Stomatal conductance (Gs); (H) Transpiration rate (Tr). Data are presented as mean ± standard error (SE) of three biological replicates. Bars with different lowercase letters indicate statistically significant differences at $p < 0.05$ according to Duncan's multiple range test.

3.2 Chloroplast Ultrastructural Alterations

Transmission electron microscopy (TEM) analysis revealed that salt stress induced differential ultrastructural damage to chloroplasts in leaf mesophyll cells of the two rice cultivars. Common structural alterations included convoluted chloroplast envelopes, disorganized thylakoid grana with loose stacking, diminished starch grains, and an increased abundance of osmiophilic plastoglobules. Notably, the severity of chloroplast damage displayed clear genotypic variation between HHZ and GH3. In salt-stressed HHZ leaves, chloroplasts exhibited severe disintegration of thylakoid lamellar systems and massive accumulation of plastoglobules. By contrast, chloroplasts in GH3 retained relatively intact overall morphology and grana architecture under salt stress, indicating superior structural stability relative to HHZ.

Foliar application of Pro-Ca effectively attenuated salt-induced chloroplast structural injury in both cultivars. Pro-Ca treatment restored the ordered stacking of thylakoid grana, reduced plastoglobule accumulation, and promoted partial restoration of starch grains. The ameliorative effect of Pro-Ca on chloroplast structure was more prominent in the salt-sensitive cultivar HHZ, whereas chloroplast ultrastructure in GH3 largely recovered to near-normal levels following Pro-Ca application.

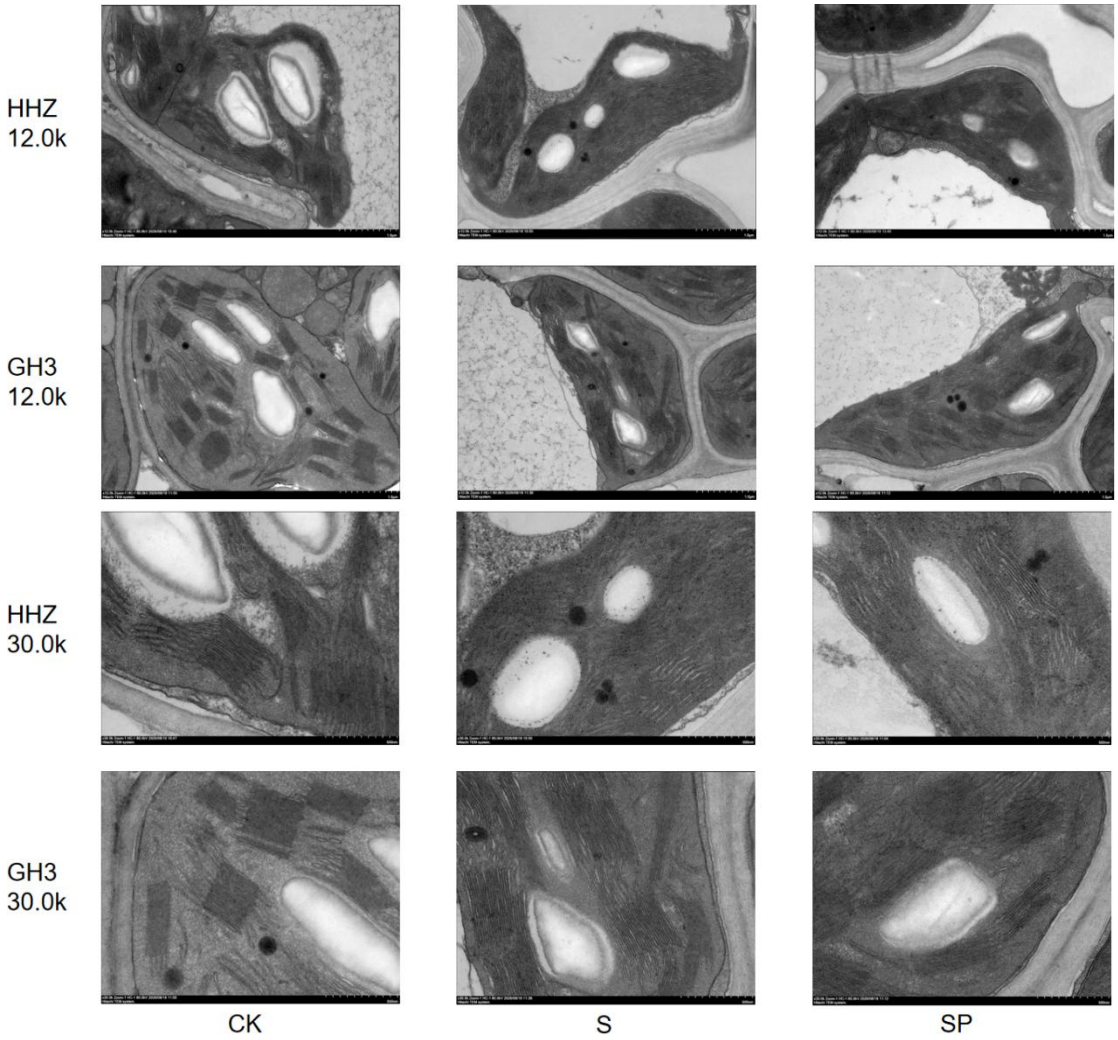


Figure 2. Transmission electron micrographs showing the effects of exogenous Pro-Ca on chloroplast ultrastructure in leaf mesophyll cells of two rice cultivars under salt stress. Magnification: 12000× (upper panel) and 3000× (lower panel).

3.3 Lipidomics Data Quality Control and Quantitative Profiling

Untargeted lipidomic analysis was performed to quantitatively profile the lipid composition of seedling leaves from the two rice cultivars

(HHZ and GH3) across all treatments. Three biological replicates were included for each experimental group.

3.3.1 Lipid Composition and Sample Quality Assessment

The leaf lipid profile of rice was dominated by three major lipid classes: glycerolipids (triacylglycerol TG and diacylglycerol DG), galactolipids (digalactosyldiacylglycerol DGDG, monogalactosyldiacylglycerol MGDG, and sulfoquinovosyldiacylglycerol SQDG), and phospholipids (phosphatidylinositol PI, phosphatidylinositol phosphate PIP, and phosphatidylglycerol PG). Collectively, these three classes accounted for over 65% of the total lipid content, whereas each of the remaining lipid classes represented less than 5% of the total (Figure 5A).

Principal component analysis (PCA) was applied to evaluate the global lipidomic variation across all samples. The first two principal components (PC1 and PC2) explained 27.2% and 13.6% of the total variance, respectively, accounting for 40.8% of the cumulative variance. Quality control (QC) samples clustered tightly with no obvious outliers, confirming high stability of the analytical system and low technical variability. For GH3, biological replicates within each treatment clustered closely and the three treatment groups were clearly separated. By contrast, inter-group separation was markedly weaker in HHZ, indicating that salt stress and Pro-Ca application exerted a stronger overall regulatory effect on the GH3 lipidome (Figure 5B). A sample correlation heatmap and hierarchical clustering analysis further validated the good intra-group reproducibility and distinct inter-group differentiation, which were consistent with the PCA findings (Figure 5C, D).

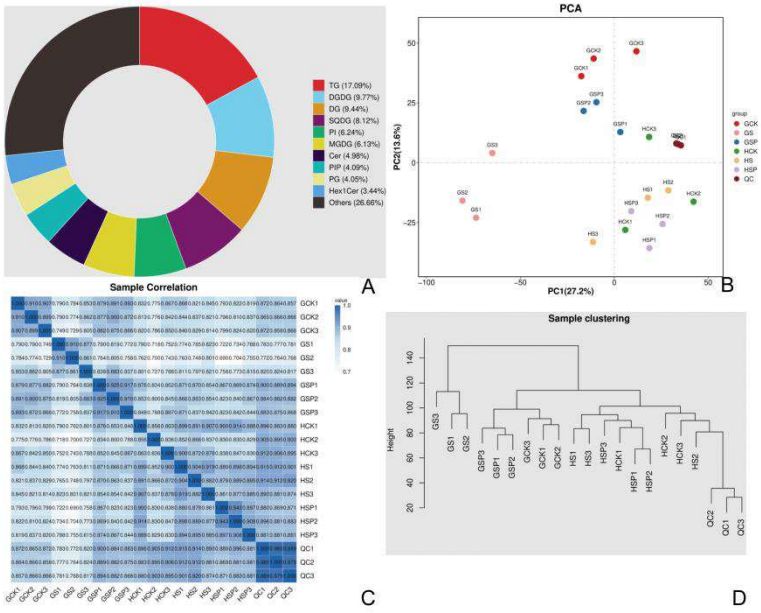


Figure 3 Lipidomic analysis profiles of rice under Pro-Ca treatment (A) Statistics of lipid composition; (B) PCA score plot of lipidome; (C) Clustering heatmap of combined positive and negative ion modes; (D) Sample clustering dendrogram of combined ion modes. Values are presented as means ± standard error (SE) of three biological replicates. Different lowercase letters above the bars indicate significant differences among treatments ($p < 0.05$).

3.3.2 Multivariate Statistical Analysis

To further identify differential lipid species between experimental groups, principal component analysis (PCA) and partial least squares discriminant analysis (PLS-DA) were conducted for each pairwise comparison. Orthogonal partial least squares discriminant analysis (OPLS-DA) coupled with permutation testing was applied to validate the robustness and reliability of the statistical models.

For the GCK vs GS comparison, PCA captured 50.4% and 17.6% of the total variance along PC1 and PC2, respectively, accounting for 68.0% cumulative variance. The two groups were completely separated along the principal component axes, with tight clustering of biological replicates within each group (Figure 6A). The corresponding PLS-DA model exhibited excellent fit and predictive performance, with R^2X = 0.874, R^2Y = 0.997, Q^2 = 0.965, and RMSEE = 0.044, supporting its suitability for subsequent differential lipid identification (Figure 6B).

For the GS vs GSP comparison, PCA explained 47.9% and 17.7% of the total variance on PC1 and PC2, respectively, with 65.6% cumulative

variance. Clear separation between the two groups and good intra-group clustering were observed (Figure 6C). The PLS-DA model showed good reliability with R^2X = 0.845, R^2Y = 0.997, Q^2 = 0.959, and RMSEE = 0.05 (Figure 6D).

For the HCK vs HS comparison, PCA accounted for 31.8% and 23.8% of the total variance along PC1 and PC2, respectively, with a cumulative variance of 55.6%. The two groups displayed a partial separation trend but did not form distinct clusters, and the magnitude of separation was smaller than that observed in the corresponding GH3 comparison (Figure 6E). The PLS-DA model showed acceptable fit with R^2X = 0.835, R^2Y = 0.995, Q^2 = 0.88, and RMSEE = 0.059 (Figure 6F).

For the HS vs HSP comparison, PCA explained 32.9% and 26.4% of the total variance on PC1 and PC2, respectively, representing 59.3% cumulative variance. The two groups were clearly discriminated with tight intra-group clustering (Figure 6G). The PLS-DA model demonstrated high reliability with R^2X = 0.86, R^2Y = 1.0, Q^2 = 0.974, and RMSEE = 0.018 (Figure 6H).

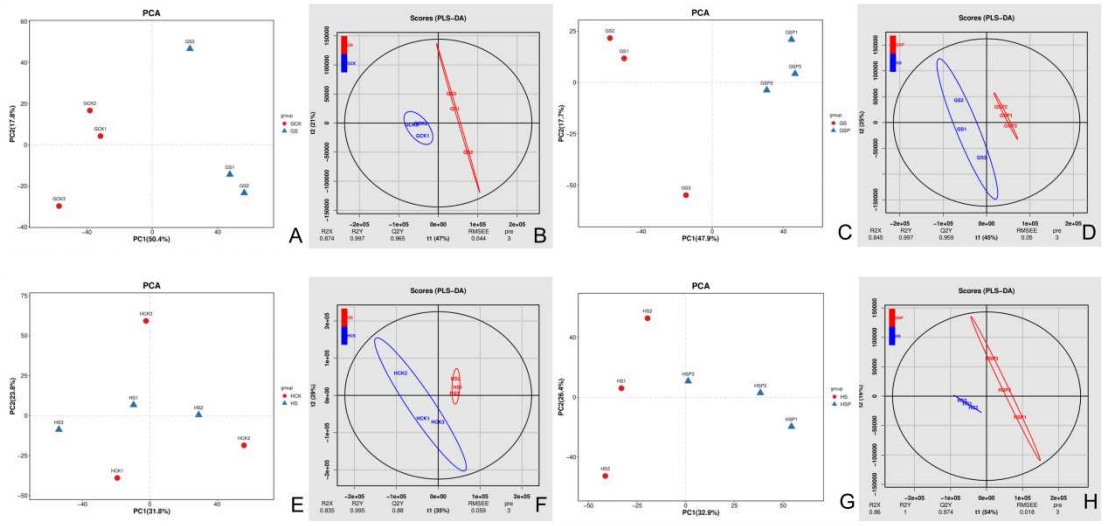


Figure 4. Multivariate statistical analysis of leaf lipid profiles in rice under salt stress and Pro-Ca treatment. (A) PCA score plot for the GCK vs GS comparison; (B) PLS-DA score plot for the GCK vs GS comparison; (C) PCA score plot for the GS vs GSP comparison; (D) PLS-DA score plot for the GS vs GSP comparison; (E) PCA score plot for the HCK vs HS comparison; (F) PLS-DA score plot for the HCK vs HS comparison; (G) PCA score plot for the HS vs HSP comparison; (H) PLS-DA score plot for the HS vs HSP comparison. Data are presented as mean ± SE of three biological replicates. Statistically significant

differences ($p < 0.05$) are indicated by different lowercase letters according to Duncan's multiple range test.

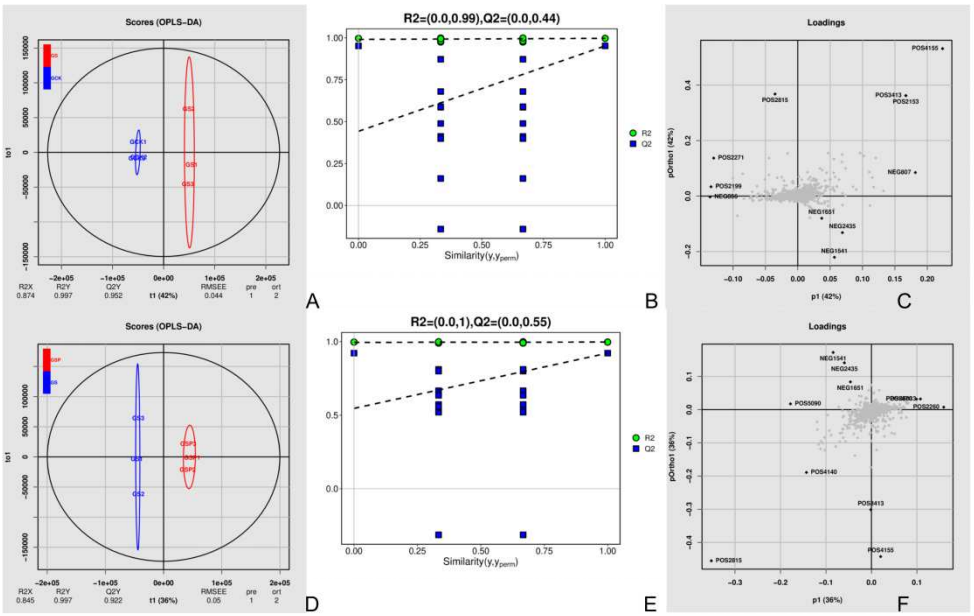
OPLS-DA models were established and validated by permutation tests for each pairwise comparison, and loading plots were generated to identify key differential lipids driving group separation.

For the GCK vs GS comparison, the OPLS-DA model yielded $R^2X = 0.874$, $R^2Y = 0.997$, and $Q^2 = 0.952$, which were highly consistent with the PLS-DA results. Permutation testing confirmed that all Q^2 values from random permutations were lower than the Q^2 of the original model, with a Q^2 regression intercept below 0.05, indicating no overfitting and high statistical reliability of the model (Figure 7A, B). The loading plot revealed that lipids on the positive side of the t1 axis were enriched under salt stress, whereas those on the negative side were more abundant in control samples. Lipids including POS4155, POS3413, and NEG807 were identified as the most prominently up-regulated species under salt stress (Figure 7C).

For the GS vs GSP comparison, the OPLS-DA model showed $R^2X = 0.845$, $R^2Y = 0.997$, and $Q^2 = 0.922$. Permutation testing verified that all randomly permuted Q^2 values were below the original model Q^2, confirming the absence of overfitting (Figure 7D, E). The loading plot indicated that lipids such as POS2260 were enriched after Pro-Ca treatment, while POS4155 remained more abundant in the salt-stressed group (Figure 7F).

For the HCK vs HS comparison, the OPLS-DA model produced $R^2X = 0.835$, $R^2Y = 0.995$, and $Q^2 = 0.897$. Permutation testing showed all random Q^2 values were lower than the original model Q^2, with no evidence of overfitting (Figure 7G, H). The loading plot demonstrated that lipids including POS2815 and POS4155 were elevated in abundance under salt stress (Figure 7I).

For the HS vs HSP comparison, the OPLS-DA model achieved $R^2X = 0.86$, $R^2Y = 1.0$, and $Q^2 = 0.927$. Permutation testing confirmed that all random Q^2 values were lower than the original value, with a Q^2 regression intercept < 0.05, supporting robust model reliability (Figure 7J, K). The loading plot showed that POS5250 was more abundant after Pro-Ca application, whereas POS4155 and POS2815 were present at higher levels in the salt-stressed group (Figure 7L).



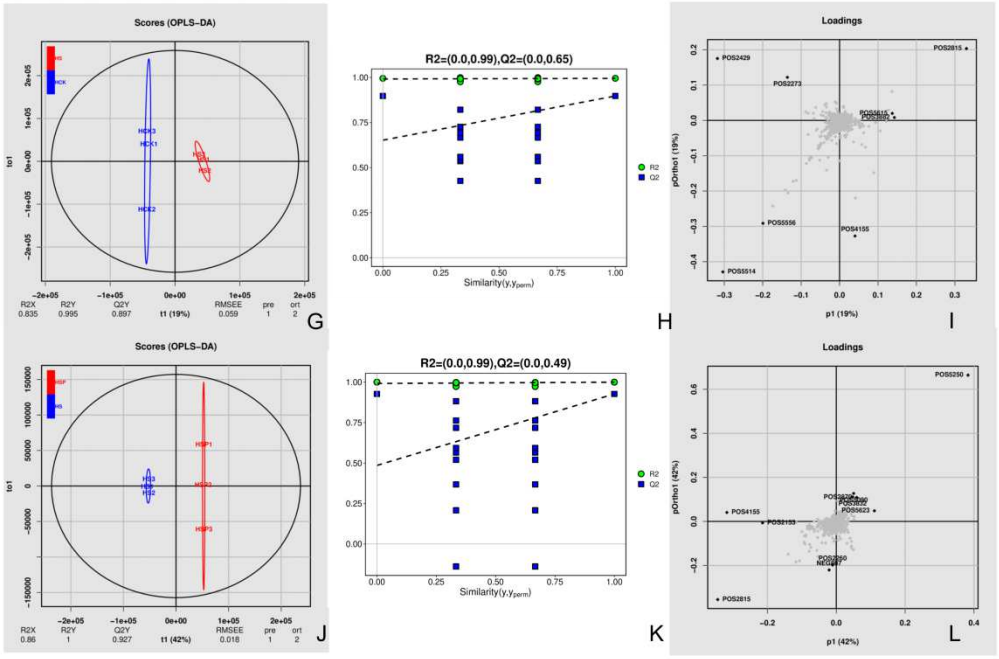


Figure 5. OPLS-DA model validation and loading analysis of leaf lipid profiles in rice under salt stress and exogenous Pro-Ca application. (A) OPLS-DA score plot for the GCK vs GS comparison; (B) Permutation test plot for the GCK vs GS OPLS-DA model; (C) Loading plot of the GCK vs GS OPLS-DA model; (D) OPLS-DA score plot for the GS vs GSP comparison; (E) Permutation test plot for the GS vs GSP OPLS-DA model; (F) Loading plot of the GS vs GSP OPLS-DA model; (G) OPLS-DA score plot for the HCK vs HS comparison; (H) Permutation test plot for the HCK vs HS OPLS-DA model; (I) Loading plot of the HCK vs HS

OPLS-DA model; (J) OPLS-DA score plot for the HS vs HSP comparison; (K) Permutation test plot for the HS vs HSP OPLS-DA model; (L) Loading plot of the HS vs HSP OPLS-DA model.

3.3.3Identification and Characterization of Differential Lipid Species

Following multivariate statistical analysis, differential lipid species in each pairwise comparison were screened by integrating the variable importance in projection (VIP) scores derived from the OPLS-DA model with the P values obtained from univariate Student's t-test. The screening criteria were defined as VIP $\geq$ 1 and P $<$ 0.05.

As summarized in Table 1, both salt stress and exogenous Pro-Ca application exerted substantially stronger regulatory effects on the GH3 lipidome compared with HHZ, as indicated by a markedly higher number of differential lipid species. This finding demonstrated a clear genotypic difference in lipid metabolic responsiveness to salt stress and Pro-Ca regulation between the two rice cultivars.

Group	Up	Down	Total
GCK VS GS	75	208	283
GS VS GSP	250	59	309
HCK VS HS	23	12	35
HS VS HSP	18	117	135

Table 1. Statistics of the number of differential lipids in different comparison groups (screening criteria: VIP $\geq$ 1, P $<$ 0.05)

Volcano plot analysis of the GCK vs GS comparison revealed that down-regulated differential lipid species markedly outnumbered up-regulated species under salt stress (Figure 8A). The top-ranked core differential lipids by VIP score included DGDG (38:12)-1, PI (16:2e/22:3), DG (18:3/18:3)-2, DGDG (18:3/20:8)-1, DG (18:3/18:2)-1, DG (18:2/18:2), and PIP (16:0/16:0), representing core biomarkers of salt stress responsiveness. Notably, DGDG (18:3/22:9)-2 and DGDG (16:0/18:3)-1 also constituted important responsive lipids due to their high VIP scores, despite exhibiting non-significant abundance changes (Figure 8B). Z-score profiling demonstrated that multiple lipid species including TG, DG, PIP, and DGDG accumulated significantly under salt stress, whereas subsets of MGDG and PI species were significantly reduced (Figure 8C).

For the GS vs GSP comparison, the volcano plot showed that up-regulated differential lipid species greatly outnumbered down-regulated species following Pro-Ca application (Figure 8D). Key responsive lipids included DGDG (18:2/18:3)-1, WE (3:0/16:4), MGDG (19:1/24:9), PIP (36:3e), SQDG (33:3)-1, and PI (33:0/18:4) (Figure 8E). Z-score analysis confirmed that multiple lipid subtypes, including PG, DGDG, PI, SQDG, Cer, TG, PIP, and MGDG, were significantly restored in abundance after Pro-Ca treatment (Figure 8F).

In the HCK vs HS comparison, the volcano plot revealed a relatively small total number of differential lipids under salt stress, with slightly more up-regulated than down-regulated species (Figure 8G). The core differential lipids were dominated by TG and DG species, such as TG (18:3/18:2/18:3), DG (18:3/18:3)-1, and TG (20:3e/11:2/18:2) (Figure 8H). Z-score profiling indicated that multiple species including ST, TG, DG, PG, PI, and SPH were significantly elevated under salt stress, whereas certain DG and TG species were decreased (Figure 8I).

For the HS vs HSP comparison, the volcano plot demonstrated that down-regulated differential lipid species significantly outnumbered up-regulated species after Pro-Ca treatment (Figure 8J). Lipids with high VIP scores were mainly TG and DG species that had been induced by salt stress, and their abundances were reduced back toward baseline levels following Pro-Ca application (Figure 8K). Consistently, Z-score analysis showed that most salt-induced lipids decreased in abundance after Pro-Ca treatment, with only a small set of lipids being up-regulated (Figure 8L).

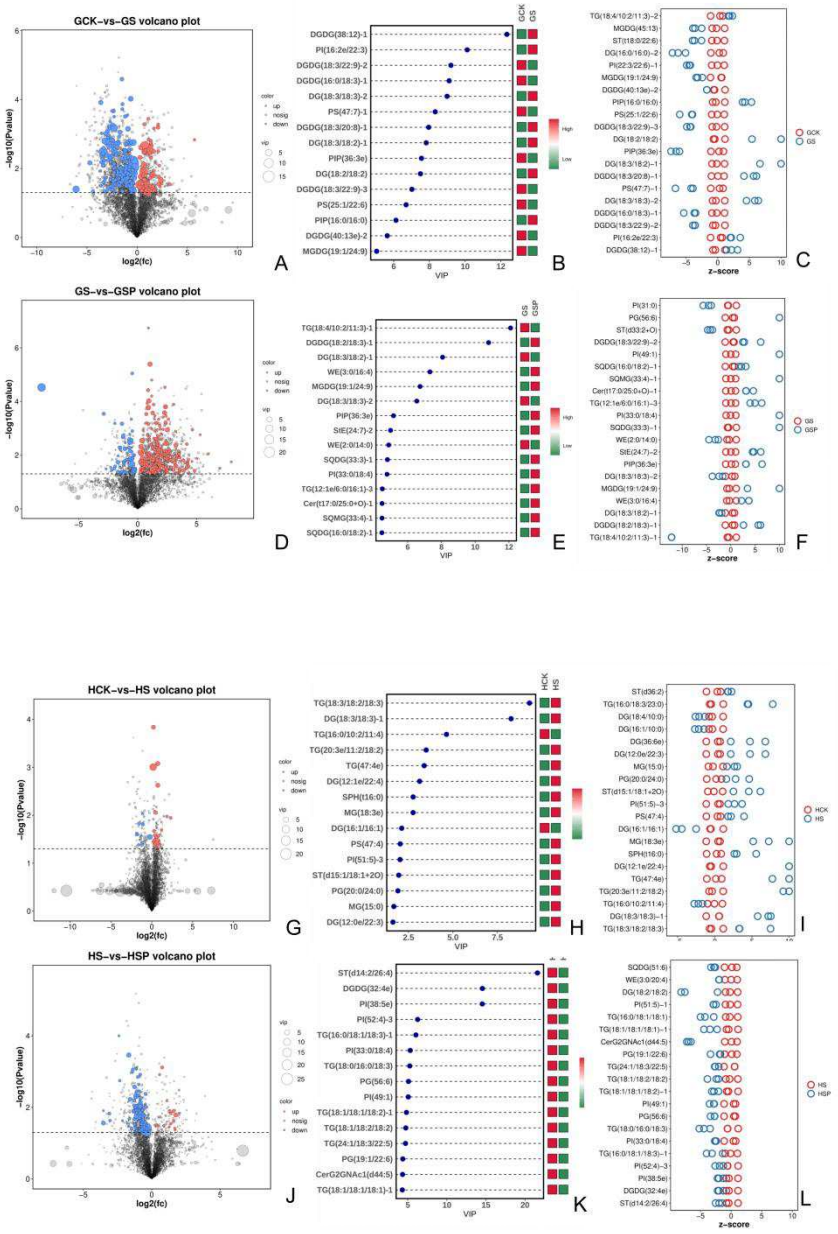


Figure 6. Differential lipid analysis of rice leaf lipid profiles under salt stress and exogenous Pro-Ca application. (A) Volcano plot for the GCK vs GS comparison; (B) VIP score plot of differential lipids for the GCK vs GS comparison; (C) Z-score profiling of differential lipids for the GCK vs GS comparison; (D) Volcano plot for the GS vs GSP comparison; (E) VIP score plot of differential lipids for the GS vs GSP comparison; (F) Z-score profiling of differential lipids for the GS vs GSP comparison; (G) Volcano plot for the HCK vs HS comparison; (H) VIP score plot of differential lipids for the HCK vs HS comparison; (I) Z-score profiling of differential lipids for the HCK vs HS comparison; (J) Volcano plot

for the HS vs HSP comparison; (K) VIP score plot of differential lipids for the HS vs HSP comparison; (L) Z-score profiling of differential lipids for the HS vs HSP comparison.

3.4 Metabolic Pathway Enrichment Analysis

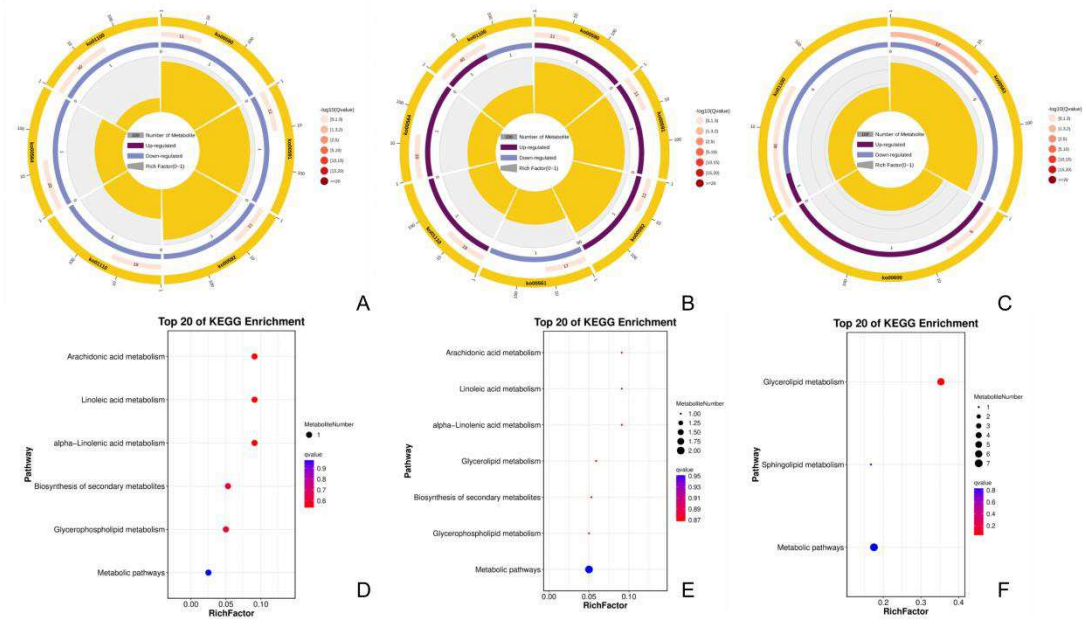
To investigate the functional consequences of salt stress and Pro-Ca-induced lipid alterations, differential lipid species were mapped onto Kyoto Encyclopedia of Genes and Genomes (KEGG) metabolic pathways, and functional enrichment analysis was performed.

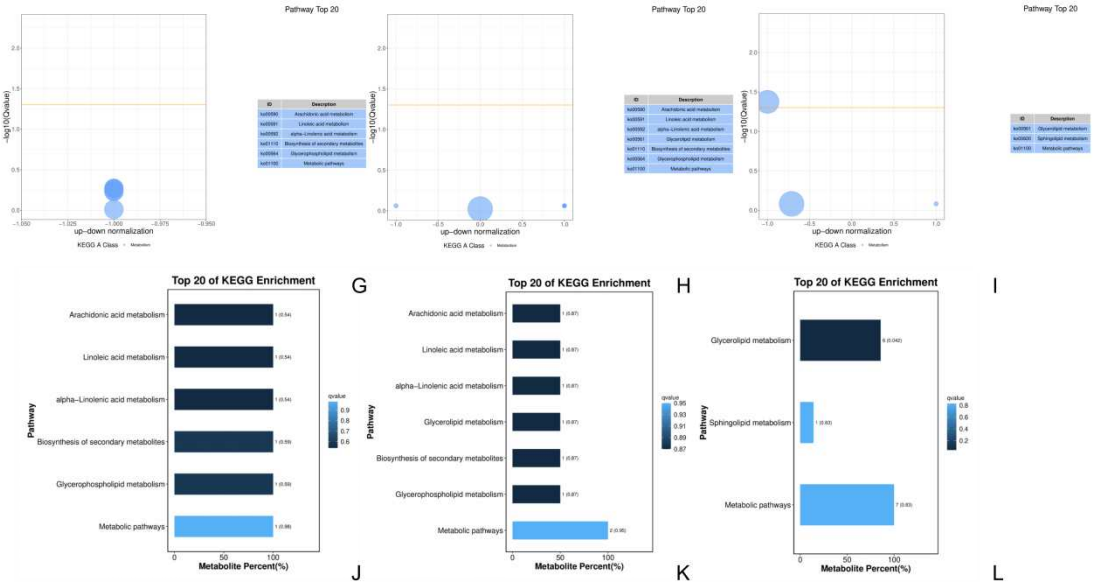
For the GCK vs GS comparison, differential lipids were annotated to 6 KEGG metabolic pathways: arachidonic acid metabolism (ko00590), linoleic acid metabolism (ko00591), α-linolenic acid metabolism (ko00592), biosynthesis of secondary metabolites (ko01110), glycerophospholipid metabolism (ko00564), and global metabolic pathways (ko01100) (Figure 9A). The global metabolic pathway harbored the highest number of differential lipid species (40). Notably, all pathways contained only one down-regulated differential lipid [PC (37:5)] and no up-regulated species (Figure 9G, 9J). Enrichment analysis revealed that none of the pathways met the threshold for statistical significance, with all adjusted P-values (Q-values) above 0.05. Arachidonic acid metabolism, linoleic acid metabolism, and α-linolenic acid metabolism exhibited relatively higher enrichment factors, representing the primary potential responsive pathways under salt stress (Figure 9D). SMPDB metabolite set enrichment analysis (MSEA) further indicated that the phospholipid biosynthesis pathway was the most highly enriched functional set (Figure 9M).

Following Pro-Ca application (GS vs GSP comparison), differential lipids mapped onto 7 KEGG metabolic pathways, with glycerolipid metabolism (ko00561) added to the aforementioned 6 pathways (Figure 9B). The global metabolic pathway contained one up-regulated and one down-regulated differential lipid, while each of the remaining pathways was annotated with one up-regulated differential lipid (Figure 9H, 9K). Consistent with the salt stress group, all KEGG pathways had Q-values > 0.05 and did not achieve significant enrichment. Arachidonic acid metabolism, linoleic acid metabolism, and α-linolenic acid metabolism remained the three pathways with the highest enrichment factors (Figure 9E). SMPDB enrichment results followed the same trend as the salt stress group, with phospholipid biosynthesis showing the highest enrichment level (Figure 9N).

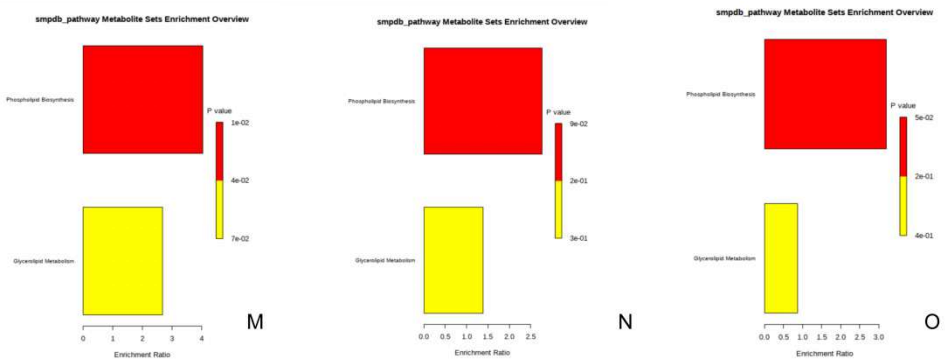
In the salt-sensitive cultivar HHZ, salt stress induced a relatively small number of differential lipids, resulting in no significantly enriched KEGG metabolic pathways. After Pro-Ca treatment (HS vs HSP comparison), differential lipids were assigned to 3 KEGG metabolic pathways: glycerolipid metabolism (ko00561, 17 annotated lipids in total), sphingolipid metabolism (ko00600, 6 annotated lipids in total), and global metabolic pathways (ko01100, 40 annotated lipids in total) (Figure 9C). Notably, glycerolipid metabolism contained 6 down-regulated differential lipids and reached significant enrichment with Q < 0.05, representing the only significantly enriched KEGG pathway in this study. Sphingolipid metabolism was annotated with one up-regulated differential lipid but did not reach statistical significance (Figure 9F, 9I, 9L). SMPDB enrichment analysis also showed a high enrichment level for the phospholipid biosynthesis pathway (Figure 9O).

Collectively, the regulatory effects of Pro-Ca on rice lipid metabolic pathways under salt stress exhibited pronounced genotypic specificity. GH3 displayed a broader range of responsive pathways but weaker enrichment intensity, with no significantly enriched KEGG pathways; phospholipid biosynthesis was identified as its core potential regulatory pathway. In contrast, HHZ showed a more focused pathway response. Glycerolipid metabolism served as the significantly enriched core pathway regulated by Pro-Ca, and the phospholipid biosynthesis pathway also exhibited a strong enrichment trend.





688



689

690

691 Figure 7. Metabolic pathway enrichment analysis of differential lipids
692 in rice seedlings under salt stress and exogenous Pro-Ca application.
693 (A) KEGG enrichment circle plot for the GCK vs GS comparison; (B) KEGG
694 enrichment circle plot for the GS vs GSP comparison; (C) KEGG
695 enrichment circle plot for the HS vs HSP comparison; (D) KEGG
696 enrichment bubble plot for the GCK vs GS comparison; (E) Differential
697 KEGG enrichment bubble plot for the GS vs GSP comparison; (F)
698 Differential KEGG enrichment bubble plot for the HS vs HSP comparison;
699 (G) KEGG differential lipid bubble plot for the GCK vs GS comparison;
700 (H) KEGG differential lipid bubble plot for the GS vs GSP comparison;
701 (I) KEGG differential lipid bubble plot for the HS vs HSP comparison;

(J) Enrichment bar plot for the GCK vs GS comparison; (K) Enrichment bar plot for the GS vs GSP comparison; (L) Enrichment bar plot for the HS vs HSP comparison; (M) KEGG metabolite set enrichment analysis (MSEA) plot for the GCK vs GS comparison; (N) MSEA plot for the GS vs GSP comparison; (O) MSEA plot for the HS vs HSP comparison.

Collectively, the response patterns of lipid metabolic pathways under salt stress exhibited pronounced genotypic divergence between the two rice cultivars. The salt-tolerant cultivar GH3 activated a broader spectrum of responsive pathways, including glycerophospholipid metabolism, fatty acid metabolism, and glycerolipid metabolism, although none of these pathways reached statistical significance at the KEGG annotation level. At the SMPDB functional set level, phospholipid biosynthesis was identified as the core potential regulatory pathway in GH3. In contrast, the salt-sensitive cultivar HHZ displayed a more concentrated pathway response. Salt stress alone induced too few differential lipids to drive significant pathway enrichment in HHZ, whereas Pro-Ca treatment triggered significant enrichment exclusively in the glycerolipid metabolism pathway ($Q < 0.05$), which represented the only significantly enriched KEGG pathway in this study.

Notably, the phospholipid biosynthesis pathway consistently showed high enrichment at the SMPDB level in both cultivars, indicating that this pathway constitutes a shared functional target through which Pro-Ca mitigates salt stress-induced lipid damage. By contrast, glycerolipid metabolism represents a cultivar-specific regulatory node of Pro-Ca action in HHZ. This divergence at the pathway level is in good agreement with the differences in the magnitude of lipid remodeling (283 differential lipid species in GH3 versus 35 in HHZ) and the distinct repair modes between the two cultivars: GH3 adopts a multi-pathway up-regulation repair strategy, while HHZ relies on targeted modulation of glycerolipid metabolism.

四、Discussion

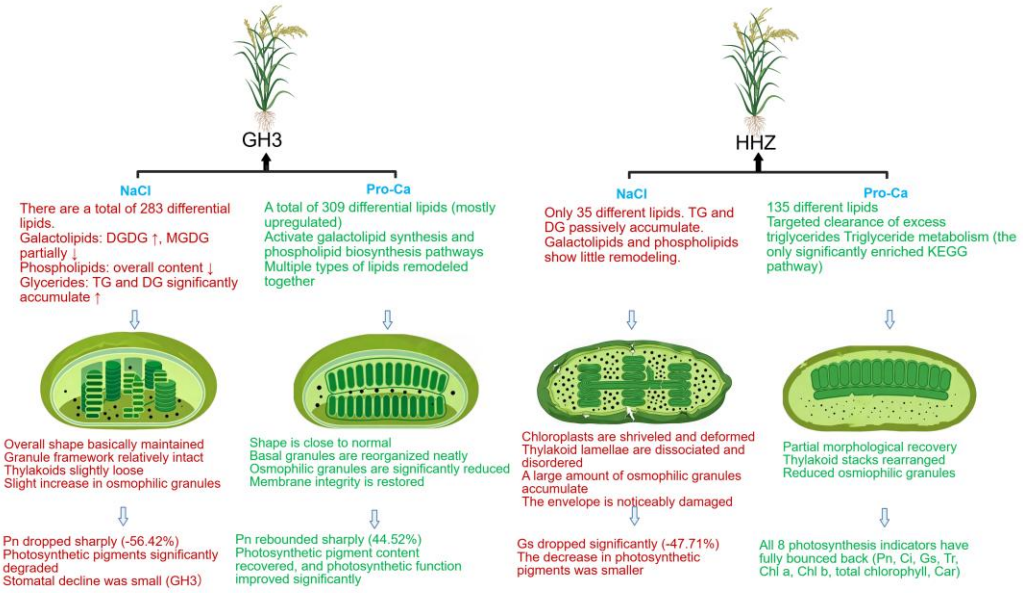


Figure 8 Schematic diagram of the mechanism underlying prohexadione-calcium alleviation of salt stress in rice via the “lipid metabolism – chloroplast structure – photosynthetic function” cascade

4.1Salt Stress-Induced Lipid Metabolic Remodeling and the Alleviating Effect of Pro-Ca

Membrane lipid remodeling serves as a core salt-tolerance adaptive mechanism for plants to maintain membrane fluidity and structural integrity(Guo et al., 2019).Untargeted lipidomic analysis in this study revealed that salt stress significantly induced lipidome remodeling in rice leaves. The number of differential lipid species was far greater in GH3 (283 species) than in HHZ (35 species), indicating that the salt-tolerant cultivar possesses a more active and broader lipid regulatory network and can actively adapt to salt stress through systematic lipid metabolic adjustment. This pattern has been widely validated in comparative studies of plants with contrasting salt tolerance, such as *Salicornia europaea* and sorghum: salt-tolerant germplasms generally exhibit stronger membrane lipid remodeling capacity and maintain the stability of cellular compartmentalized structures via coordinated regulation of multiple lipid classes(Ge et al., 2022; Yang et al., 2025).

Under salt stress, neutral glycerolipids including triacylglycerol (TG) and diacylglycerol (DG) were significantly accumulated in leaves

of both cultivars, with a greater accumulation magnitude in GH3. Accumulating evidence confirms that massive TG accumulation in plants under abiotic stress serves as a temporary reservoir for free fatty acids, preventing lipotoxicity and membrane lipid peroxidation induced by excess free fatty acids. Meanwhile, it modulates cellular osmotic pressure and enhances water retention, representing a conservative adaptive strategy for plants in response to osmotic stress(Mei-zhen ZHANG 2023; Tamanna et al., 2024).However, comparative studies between wild rice and cultivated rice indicate that excessive accumulation of glycerolipids is more likely a manifestation of metabolic damage caused by salt stress rather than an active adaptive strategy(Tamanna et al., 2024).In this study, the more prominent dynamic response of glycerolipids in GH3 is consistent with its stronger damage repair capacity and membrane homeostasis regulation ability.

Chloroplast galactolipids are the core skeletal components of thylakoid membranes, accounting for the vast majority of total thylakoid membrane lipids. Changes in their composition directly affect the assembly of photosynthetic complexes and the functional stability of photosystems(Li et al., 2024; Wang et al., 2014).In this study, salt stress significantly elevated digalactosyldiacylglycerol (DGDG) content and induced a partial reduction in monogalactosyldiacylglycerol (MGDG) in GH3, resulting in an increased DGDG/MGDG ratio. OsMGD1 is a key enzyme regulating galactolipid biosynthesis in rice. Previous studies have confirmed that OsMGD1-overexpressing lines stabilize thylakoid membrane structure by increasing the total contents of MGDG and DGDG, leading to a 27.5% increase in net photosynthetic rate(Li et al., 2024; RiceData, 2026).Studies on sorghum under salt stress have also demonstrated that an elevated DGDG/MGDG ratio enhances the structural stability of the membrane bilayer and alleviates salt stress-induced damage to thylakoid membranes, representing an important membrane adaptive mechanism of plants in response to salt stress(Ge et al., 2022).In contrast, the magnitude of change in chloroplast galactolipids was smaller in HHZ, indicating insufficient thylakoid membrane lipid remodeling capacity, which may serve as an important molecular basis for the higher susceptibility of chloroplast structure to damage under salt stress in this cultivar.

In terms of the phospholipid profile, salt stress reduced the content of phosphatidylcholine (PC) in both cultivars, while up-regulating signaling phospholipids such as phosphatidylinositol phosphate (PIP). As the primary structural phospholipid of the biological membrane bilayer, decreased PC content leads to reduced membrane fluidity and structural stability. In contrast, PIP functions as a second messenger involved in salt stress signal

transduction(Mansour, 2013; Yang et al., 2025).Integrated transcriptomic and lipidomic analysis in *Salicornia europaea* has confirmed that both the phosphatidylinositol signaling pathway and glycerophospholipid metabolic pathway are significantly activated under salt stress, which together constitute the core regulatory network for maintaining plasma membrane structural stability(Yang et al., 2025).Studies on Kentucky bluegrass (*Poa pratensis*) have also demonstrated that the optimization degree of phospholipid components under salt stress is directly correlated with the salt tolerance level of plants(Zuo et al., 2023).In the present study, the more extensive phospholipid remodeling observed in GH3 is consistent with its greater cellular structural stability, and vice versa.

Foliar application of Pro-Ca significantly reversed salt stress-induced lipid metabolic disorders, restoring the overall leaf lipid profile to the control level. In terms of the number of differential lipids, 309 Pro-Ca-responsive differential lipids were identified in GH3, predominantly up-regulated, indicating that Pro-Ca repairs salt stress-induced membrane lipid damage by activating a broad spectrum of lipid synthesis pathways. In contrast, 135 differential lipids were detected in HHZ, predominantly down-regulated, suggesting that its alleviating effect focuses more on clearing toxic lipids excessively accumulated under salt stress. This difference is consistent with the salt injury characteristics of the two cultivars: the salt-tolerant cultivar has a wider range of damage but strong repair potential, while the salt-sensitive cultivar has concentrated injury sites and a single repair pathway. Exogenous choline alleviates salt stress injury in Kentucky bluegrass by promoting phospholipid synthesis(Zuo et al., 2023).and our results also confirm that Pro-Ca possesses a similar lipid homeostasis regulatory capacity.

4.2 Protective Effect of Lipid Homeostasis Regulation on Chloroplast Ultrastructure

The structural integrity of chloroplast thylakoid membranes is highly dependent on the homeostasis of membrane lipid components, and dynamic remodeling of lipid metabolism directly determines the stability of chloroplast ultrastructure. Transmission electron microscopy (TEM) observations in this study revealed that the difference in the severity of chloroplast structural damage between the two cultivars was highly consistent with the difference in their lipid metabolic responsiveness. GH3 actively maintained membrane

structural stability via adjustment of galactolipid composition (elevated DGDG/MGDG ratio) and coordinated remodeling of phospholipids and signaling lipids, thus preserving the overall chloroplast morphology and grana lamella framework. In contrast, HHZ exhibited limited membrane lipid remodeling capacity and only passively accumulated neutral glycerolipids, failing to effectively sustain thylakoid membrane structure, which resulted in more severe damage including thylakoid lamella dissociation and osmiophilic granule aggregation.

Foliar application of Pro-Ca effectively ameliorated salt stress-induced chloroplast structural damage by regulating lipid homeostasis. In terms of the compositional profile of differential lipids, 309 Pro-Ca-responsive differential lipids were identified in GH3, with up-regulated lipids accounting for the majority. This result indicated that Pro-Ca could activate the biosynthetic pathways of multiple lipid classes such as galactolipids and phospholipids, comprehensively restoring the membrane lipid composition of thylakoid membranes and plasma membranes, and providing a material basis for chloroplast structural recovery. After Pro-Ca treatment, differential lipids in HHZ were predominantly down-regulated. Its alleviating effect was mainly exerted by scavenging excessively accumulated neutral glycerolipids and reducing lipotoxic injury to chloroplast membranes, thereby mitigating structural disruption.

The repair effects in the two cultivars were highly consistent with their respective lipid regulatory modes. GH3 activated lipid biosynthesis through multiple pathways, restoring its chloroplast structure to a level close to normal. The targeted glycerolipid clearance regulatory mode in HHZ also significantly improved thylakoid grana stacking and alleviated osmiophilic granule accumulation. These results directly validated the causal relationship of *lipid metabolism remodeling→chloroplast structure protection*. A previous study showing that heterologous overexpression of the rice MGD synthase gene in tobacco enhanced salt tolerance by increasing galactolipid content(Wang et al., 2014), also corroborated the critical role of galactolipid biosynthesis in chloroplast structural stability and plant salt tolerance from the perspective of genetic functional verification.

4.3 Alleviating Effect of Chloroplast Structural Restoration on Photosynthetic Function Impairment

Chloroplasts are the core sites of photosynthesis in plants, and the integrity of their ultrastructure directly determines the normal

operation of photosynthetic function. Salt stress inhibits plant photosynthesis through both stomatal and non-stomatal limitation pathways(Qi et al., 2026).The difference in photosynthetic inhibition patterns between the two cultivars in this study is essentially an external manifestation of differences in chloroplast structural damage severity and stress regulatory strategies..

GH3 exhibited a greater reduction in net photosynthetic rate, but a significantly smaller decrease in stomatal conductance than HHZ, indicating a higher contribution of non-stomatal limitation to its photosynthetic inhibition, which was mainly attributed to photosynthetic pigment degradation and chloroplast structural damage. However, GH3 alleviated chloroplast oxidative damage by actively down-regulating photosynthetic activity and reducing reactive oxygen species production, representing an active stress adaptation strategy. In contrast, HHZ had weak stomatal regulatory capacity and maintained a relatively higher gas exchange level in the short term, but exacerbated ion toxicity and oxidative damage, which eventually led to more severe disruption of chloroplast structure and sustained impairment of photosynthetic function(Song et al., 2023; Yang, 2018).Comparative studies between wild rice and cultivated rice have also confirmed that salt-tolerant germplasms reduce water loss by actively regulating stomatal aperture, while maintaining the activity of key carbon assimilation enzymes to balance photosynthetic efficiency and stress damage, thus forming differentiated adaptive strategies(Yun et al., 2025).

After Pro-Ca treatment, photosynthetic function was significantly improved in both cultivars, and the repair effect on photosynthetic function was highly consistent with the repair degree of chloroplast ultrastructure. The significant restoration of chloroplast membrane structure and grana stacking in GH3 directly supported a large recovery of net photosynthetic rate by 44.52%. The partial restoration of chloroplast structure in HHZ also led to a comprehensive recovery of 8 photosynthetic indicators. These results fully validated the cascade regulatory pathway of *lipid homeostasis→chloroplast structure→photosynthetic function*.

4.4 Lipid–Structure–Function Regulatory Mechanism and Genotypic Specificity of Prohexadione-Calcium in Alleviating Salt Stress in Rice

Accumulating studies have confirmed that Pro-Ca alleviates salt stress injury in plants through multiple pathways, including activating antioxidant defense, maintaining ion homeostasis, and protecting photosynthetic function(Deng, 2024; Liang et al., 2025; Liu et al., 2025).Transcriptomic studies in rice have also confirmed

that Pro-Ca regulates the expression of antioxidant- and photosynthesis-related genes at the transcriptional level(Li et al., 2023).However, its regulatory mechanism on lipid metabolism has not been reported previously. This study systematically elucidated the cascade regulatory mechanism of Pro-Ca in alleviating salt stress in rice: foliar application of Pro-Ca first regulates lipid metabolic remodeling in leaves and maintains biological membrane structural stability by restoring membrane lipid composition; it further preserves the integrity of chloroplast ultrastructure and restores the ordered stacking of thylakoid grana; ultimately, it alleviates photosynthetic inhibition and improves the photosynthetic capacity of rice seedlings under salt stress.In this study, GH3 inherently possessed a strong foundation for lipid homeostasis regulation and could initiate extensive membrane lipid remodeling responses under salt stress. After Pro-Ca treatment, multiple lipid biosynthetic pathways, including those for galactolipids, phospholipids, and glycerolipids, were further activated. Through the coordinated regulation of multiple lipid classes, the membrane lipid system was comprehensively repaired and chloroplast ultrastructure was stabilized, ultimately driving a substantial recovery in photosynthetic rate. SMPDB pathway enrichment analysis revealed that the phospholipid biosynthesis pathway was the core regulatory target of Pro-Ca in GH3.In contrast, HHZ exhibited weak intrinsic lipid regulatory capacity, and the most prominent metabolic disorder under salt stress was excessive glycerolipid accumulation. The regulatory effect of Pro-Ca on HHZ mainly targeted the clearance of excessively accumulated neutral glycerolipids such as TG and DG to alleviate lipotoxic injury, thereby improving chloroplast structure and photosynthetic function. Glycerolipid metabolism was the only significantly enriched KEGG pathway under Pro-Ca regulation in HHZ, and also represented a cultivar-specific regulatory target. This also explained why the glycerolipid pathway showed the highest enrichment level in HHZ, but the overall photosynthetic recovery amplitude was smaller than that in GH3: repair of a single pathway was insufficient to fully compensate for the overall damage to the membrane lipid system.

In addition, the up-regulation of sphingolipids such as ceramide (Cer) after Pro-Ca treatment suggests that signaling lipids may be involved in the regulatory process of Pro-Ca against salt stress. As a signaling molecule, Cer is widely involved in plant stress signal transduction(Guo et al., 2019; Yang et al., 2025).A classic study by DeWald et al. in *Arabidopsis thaliana* confirmed that salt stress rapidly induces the biosynthesis of phosphatidylinositol 4,5-

bisphosphate (PIP_2). PIP_2 is subsequently hydrolyzed to produce inositol 1,4,5-trisphosphate (IP_3), and IP_3 production is closely correlated with intracellular Ca^{2+} mobilization. This work constituted an early classic validation of the core cascade of the phosphatidylinositol (PI) signaling pathway, namely the "PIP_2 → IP_3 → Ca^{2+} signaling" axis (DeWald et al., 2001).This study validates that the phosphatidylinositol signaling pathway serves as a central hub bridging salt stress signal perception, second messenger generation and transduction, and the ultimate regulation of downstream salt tolerance responses in plants. Based on this, we hypothesize that Pro-Ca may indirectly modulate sphingolipid and phosphatidylinositol signaling via regulating the gibberellin signaling pathway, thereby triggering downstream lipid remodeling and stress defense responses. Nevertheless, the detailed molecular mechanism underlying this signaling cascade remains to be further verified.

This study systematically dissected the regulatory effects of Pro-Ca on lipid metabolism, chloroplast ultrastructure, and photosynthetic function in rice seedlings under salt stress, and identified the genotypic differences between the two cultivars. However, several limitations still exist. First, the study only focused on lipid responses in leaves at the seedling stage, and did not cover roots, the core tissue for stress perception and ion transport, nor did it perform dynamic tracking across different growth stages. Therefore, it is difficult to fully reflect the regulatory pattern of Pro-Ca on salt stress across the entire rice growth period. Second, the study only revealed the pattern of lipid changes at the metabolic level, and did not validate the molecular regulatory mechanism of lipid biosynthesis pathways by combining transcriptomic analysis, key enzyme activity assays and other approaches. The specific roles of key lipid biosynthesis enzymes such as OsMGD1 in the Pro-Ca regulatory pathway remain unclear(Li et al., 2024).Future studies may integrate multi-omics technologies to further identify the key genes and signaling pathways involved in the regulation of lipid metabolism by Pro-Ca, and clarify its molecular regulatory network. Meanwhile, multi-site field trials should be conducted to verify its application efficacy, providing a more solid theoretical basis for the precision application of Pro-Ca in stress-resistant rice cultivation in saline-alkali soils.

五、Conclusion

In this study, two rice cultivars, the salt-sensitive cultivar Huanghuazhan (HHZ) and the salt-tolerant cultivar Guanghong No. 3 (GH3), were used as experimental materials. Combined with non-

targeted lipidomics, transmission electron microscopy (TEM) observation of ultrastructure, and photosynthetic physiological measurement, we systematically elucidated the mechanism by which prohexadione-calcium (Pro-Ca) alleviates photosynthetic salt damage in rice seedlings by regulating leaf lipid homeostasis and maintaining chloroplast ultrastructural integrity. The main conclusions are as follows:

1.There are significant genotypic differences in rice responses to salt stress. The salt-tolerant cultivar GH3 possesses a stronger membrane lipid remodeling capacity. A total of 283 differential lipids were identified under salt stress. Through the coordinated response of multiple lipid classes, including galactolipid composition adjustment (DGDG up-regulation and partial MGDG down-regulation), phospholipid metabolic remodeling, and moderate glycerolipid accumulation, GH3 actively maintained the grana lamella framework and overall morphological stability of chloroplasts. Its photosynthetic inhibition was dominated by non-stomatal limitation (significant degradation of photosynthetic pigments). In contrast, the salt-sensitive cultivar HHZ exhibited limited lipid regulatory capacity, with only 35 differential lipids detected. Its core feature was the passive excessive accumulation of neutral glycerolipids such as TG and DG, accompanied by more severe chloroplast damage including thylakoid lamella dissociation and osmiophilic granule aggregation. Its photosynthetic inhibition was dominated by stomatal limitation.

2.Pro-Ca alleviates salt stress injury through the cascade pathway of "lipid homeostasis → chloroplast structure → photosynthetic function". Foliar application of Pro-Ca preferentially reshaped the leaf lipid profile and restored membrane lipid composition disorder. It further restored the ordered stacking of thylakoid grana in chloroplasts, reduced osmiophilic granule accumulation, and maintained chloroplast structural integrity. Ultimately, it improved photosynthetic gas exchange parameters and photosynthetic pigment content, and effectively alleviated photosynthetic inhibition. These results fully validated the cascade regulatory pathway from molecular metabolism to cellular structure and then to physiological function.

3.The regulatory effect of Pro-Ca shows significant genotypic specificity. In GH3, Pro-Ca activated multiple lipid biosynthetic pathways such as galactolipid and phospholipid pathways, and

comprehensively repaired the membrane lipid system through the synergistic action of multiple lipid classes. A total of 309 differential lipids were identified, predominantly up-regulated, which ultimately drove a substantial recovery of net photosynthetic rate (Pn) by 44.52%. The phospholipid biosynthesis pathway was its core potential regulatory target. In HHZ, Pro-Ca mainly targeted the clearance of excessively accumulated glycerolipids. Glycerolipid metabolism was the only significantly enriched KEGG pathway ($Q < 0.05$). Although it achieved a comprehensive recovery of 8 photosynthetic indicators, the overall repair effect was weaker than that in GH3.

4.This study revealed a novel lipid metabolic mechanism of Pro-Ca in regulating rice salt stress responses, and provides an important theoretical basis for the rational application of plant growth regulators in stress-resistant rice cultivation in saline-alkali soils. Future studies can further dissect its molecular regulatory network by combining transcriptome sequencing and key enzyme activity assays, and conduct multi-site field trials to verify its field application efficacy.

List of abbreviations

ANOVA, one-way analysis of variance

Car, carotenoids

Cer, ceramide

Chl a, chlorophyll a

Chl b, chlorophyll b

Ci, intercellular CO_2 concentration

CK, control

DG, diacylglycerol

DGDG, digalactosyldiacylglycerol

Fv/Fm, maximum photochemical quantum yield of PSII

Fv/Fo, PSII potential activity

GH3, Guanghong No. 3

Gs, stomatal conductance

HHZ, Huanghuazhan

KEGG, Kyoto Encyclopedia of Genes and Genomes

MGDG, monogalactosyldiacylglycerol

MSEA, metabolite set enrichment analysis

MS/MS, tandem mass spectrometry

MTBE, methyl tert-butyl ether

m/z, mass-to-charge ratio

OPLS-DA, orthogonal partial least squares discriminant analysis

PA, phosphatidic acid

PAR, photosynthetically active radiation

PC, phosphatidylcholine

PCA, principal component analysis

PE, phosphatidylethanolamine

PG, phosphatidylglycerol;

PI, phosphatidylinositol

PIP, phosphatidylinositol phosphate

PLS-DA, partial least squares discriminant analysis

Pn, net photosynthetic rate

Pro-Ca, prohexadione calcium

PS, phosphatidylserine

PSII, photosystem II

QC, quality control

RMSEE, root mean square error of estimation

RT, retention time

SD, standard deviation

SE, standard error

SMPDB, Small-Molecule Pathway Database

SPH, sphingolipid

SQDG, sulfoquinovosyldiacylglycerol

ST, sterol

TEM, transmission electron microscopy

TG, triacylglycerol

Tr, transpiration rate

UHPLC, ultra-high performance liquid chromatography

VIP, variable importance in projection

WE, wax ester.

Declarations

Ethics approval and consent to participate

Not applicable.

Consent for publication

Not applicable.

Availability of data and materials

The lipidomics data (BioProject accession: PRJCA077153; OMIX accession: OMIX022029) have been deposited in the Open Archive for Miscellaneous Data (OMIX) of the China National Center for Bioinformation (CNCB). The dataset is under embargo and will be publicly released automatically upon publication of the corresponding article. After the release, it can be accessed via the following link: https://ngdc.cncb.ac.cn/bioproject/browse/PRJCA077153. Prior to the release, the data are restricted to the submitters and are not accessible to the public.

Among them, the Guanghong No.3 seeds come from the Guangdong Academy of Agricultural Sciences, and the Huahuazhan seeds come from Shenzhen Jingulong Seed Co., Ltd.

Competing interests

The authors declare that they have no competing interests.

Funding

Guangdong Provincial Education Department Key Field Special Project for Colleges and Universities, No.2021ZdZX4027

Author contributions

Y.Q. Responsible for manuscript writing, investigation, data collation and formal analysis. X.W. Assisted in investigation and sample preparation. Z.C. Assisted in investigation and data sorting. H.N. Assisted in result verification and literature collation. Y.Z. Assisted in chart drawing and data validation. G.S. Assisted in experiment implementation and sample testing. H.C. Assisted in manuscript proofreading and revision. All authors participated in the preparation, writing and revision of the manuscript and approved the final submitted version.

Acknowledgements

Not applicable.

Ahmadi, N., Negrão, S., Katsantonis, D., Frouin, J., Ploux, J., Letourmy, P., Droc, G., Babo, P., Trindade, H., Bruschi, G., Greco, R., Oliveira, M. M., Piffanelli, P., & Courtois, B. (2011). Targeted association analysis identified japonica rice varieties achieving Na+/K+ homeostasis without the allelic make-up of the salt tolerant indica variety Nona Bokra. *Theoretical and Applied Genetics*, *123*(6), 881–895. https://doi.org/10.1007/s00122-011-1634-4

Block, M. A. D., A.-J.; Joyard, J.; Douce, R. (1983). Preparation and characterization of membrane fractions enriched in outer and inner envelope membranes from spinach chloroplasts. II. Biochemical characterization. *Journal of Biological Chemistry*, *258*(21), 13281–13286. https://doi.org/ 10.1016/S0021-9258(17)44113-5

Borrell, J. H. D., Òscar; Keough, Kevin M.W. (2016). *Membrane Protein – Lipid Interactions: Physics and Chemistry in the Bilayer* (1st ed. 2016 ed.). Springer International Publishing. https://doi.org/10.1007/978-3-319-30277-5

Deng, P. K., Aaqil；Zhou, Hong；Lu, Xu；Zhao, Hui；Du, Ying；Wang, Yifan；Feng, Najia；Zheng, Dianfeng. (2024). Application of prohexadione-calcium priming affects Brassica napus L. seedlings by regulating morph-physiological characteristics under salt stress. *PeerJ*, *12*, e17312. https://doi.org/ 10.7717/peerj.17312

DeWald, D. B., Torabinejad, J., Jones, C. A., Shope, J. C., Cangelosi, A. R., Thompson, J. E., Prestwich, G. D., & Hama, H. (2001). Rapid Accumulation of Phosphatidylinositol 4,5-Bisphosphate and Inositol 1,4,5-Trisphosphate Correlates with Calcium Mobilization in Salt-Stressed Arabidopsis. *Plant Physiology*, *126*(2), 759–769. https://doi.org/10.1104/pp.126.2.759

Du, Y., Zhao, H., Feng, N., Zheng, D., Khan, A., Zhou, H., Deng, P., Wang, Y., Lu, X., & Jiang, W. (2024). Alginate Oligosaccharides Alleviate Salt Stress in Rice Seedlings by Regulating Cell Wall Metabolism to Maintain Cell Wall Structure and Improve Lodging Resistance. *Plants*, *13*(9), 1215.

Fahad, S., Noor, M., Adnan, M., Khan, M. A., Rahman, I. U., Alam, M., Khan, I. A., Ullah, H., Mian, I. A., Hassan, S., Saud, S., Bakhat, H. F., Hammad, H. M., Ahmad, S., & Nasim, W. (2019). Chapter 28 - Abiotic Stress and Rice Grain Quality. In M. Hasanuzzaman, M. Fujita, K. Nahar, & J. K. Biswas (Eds.), *Advances in Rice Research for Abiotic Stress Tolerance* (pp. 571–583). Woodhead Publishing. https://doi.org/https://doi.org/10.1016/B978-0-12-814332-2.00028-9

Feng, N., Yu, M., Li, Y., Jin, D., & Zheng, D. (2021). Prohexadione-calcium alleviates saline-alkali stress in soybean seedlings by improving the photosynthesis and up-regulating antioxidant defense. *Ecotoxicology and Environmental Safety*, *220*, 112369. https://doi.org/https://doi.org/10.1016/j.ecoenv.2021.112369

Ge, S., Liu, D., Chu, M., Liu, X., Wei, Y., Che, X., Zhu, L., He, L., & Xu, J. (2022). Dynamic and adaptive membrane lipid remodeling in leaves of sorghum under salt stress. *The Crop Journal*, *10*(6), 1557–1569. https://doi.org/https://doi.org/10.1016/j.cj.2022.03.006

Gigon, A. M., Ana-Rita; Laffray, Daniel; Zuily-Fodil, Yasmine; Pham-Thi, Anh-Thu. (2004). Effect of drought stress on lipid metabolism in the leaves of Arabidopsis thaliana (ecotype Columbia). *Annals of Botany*, *94*(3), 345–351. https://doi.org/10.1093/aob/mch150

Guo, Q., Liu, L., & Barkla, B. J. (2019). Membrane Lipid Remodeling in Response to Salinity. *International Journal of Molecular Sciences*, *20*(17), 4264.

Jiang, D. X., Chu, X., Li, M., Hou, J. J., Tong, X., Gao, Z. P., & Chen, G. X. (2020). Exogenous spermidine enhances salt-stressed rice photosynthetic performance by stabilizing structure and function of chloroplast and thylakoid membranes. *Photosynthetica*, *58*(1), 61–71. https://doi.org/10.32615/ps.2019.160

Kalisch, B., Dörmann, P., & Hölzl, G. (2016). DGDG and Glycolipids in Plants and Algae. In Y. Nakamura & Y. Li-Beisson (Eds.), *Lipids in Plant and Algae Development* (pp. 51–83). Springer International Publishing. https://doi.org/10.1007/978-3-319-25979-6_3

Kolomeichuk, L. V., Efimova, M. V., Zlobin, I. E., Kreslavski, V. D., Murgan, O. g. K., Kovtun, I. S., Khripach, V. A., Kuznetsov, V. V., & Allakhverdiev, S. I. (2020). 24-Epibrassinolide alleviates the toxic effects of NaCl on photosynthetic processes in potato plants. *Photosynthesis Research*, *146*(1), 151–163. https://doi.org/10.1007/s11120-020-00708-z

Landi, S., Hausman, J.-F., Guerriero, G., & Esposito, S. (2017). Poaceae vs. Abiotic Stress: Focus on Drought and Salt Stress, Recent Insights and Perspectives [Mini Review]. *Frontiers in Plant Science*, *Volume 8 - 2017*. https://doi.org/10.3389/fpls.2017.01214

Li, N., Xu, C., Li-Beisson, Y., & Philippar, K. (2016). Fatty Acid and Lipid Transport in Plant Cells. *Trends in Plant Science*, *21*(2), 145–158. https://doi.org/https://doi.org/10.1016/j.tplants.2015.10.011

Li, S., Hui, L., Li, J., Xi, Y., Xu, J., Wang, L., & Yin, L. (2024). OsMGD1-Mediated Membrane Lipid Remodeling Improves Salt Tolerance in Rice. *Plants*, *13*(11), 1474.

Li, Y., Zhou, H., Feng, N., Zheng, D., Ma, G., Feng, S., Liu, M., Yu, M., Huang, X., & Huang, A. (2023). Physiological and transcriptome analysis reveals that prohexadione-calcium promotes rice seedling's development under salt stress by regulating antioxidant processes and photosynthesis. *PLOS ONE*, *18*(6), e0286505. https://doi.org/10.1371/journal.pone.0286505

Liang, X., Dong, Y., Jiang, Q., Hou, X., Song, Y., Zhao, F., Sun, Y., Jiang, H., Fang, S., & Wang, Q. (2025). Foliar spray of prohexadione-calcium improves the adaptability of mung bean to saline-alkali stress [Original Research]. *Frontiers in Plant Science*, *Volume 16 - 2025*. https://doi.org/10.3389/fpls.2025.1681992

Liu, C., Mao, B., Yuan, D., Chu, C., & Duan, M. (2022). Salt tolerance in rice: Physiological responses and molecular mechanisms. *The Crop Journal*, *10*(1), 13–25. https://doi.org/https://doi.org/10.1016/j.cj.2021.02.010

Liu, M., Feng, N., Zheng, D., & Meng, F. (2025). Comparative Study of the Mechanisms Underlying the Effects of Prohexadione-Calcium and Gibberellin on the Morphogenesis and Carbon Metabolism of Rice Seedlings Under NaCl Stress. *Plants*, *14*(8), 1240.

Liu, Z., Ma, C., Hou, L., Wu, X., Wang, D., Zhang, L., & Liu, P. (2022). Exogenous SA Affects Rice Seed Germination under Salt Stress by Regulating Na+/K+ Balance and Endogenous GAs and ABA Homeostasis. *International Journal of Molecular Sciences*, *23*(6), 3293.

Lv, S. T., Fang; Guo, Jianchao; Jiang, Ping; Lin, Kexin; Wang, Deli; Zhang, Xiaohua; Li, Yinxin. (2021). Phosphatidylserine Synthase from Salicornia europaea Is Involved in Plant Salt Tolerance by Regulating Plasma Membrane Stability. *Plant and Cell Physiology*, *62*(1), 66–79. https://doi.org/10.1093/pcp/pcaa141

Mansour, M. M. F. (2013). Plasma membrane permeability as an indicator of salt tolerance in plants. *Biologia plantarum*, *57*(1), 1–10. https://doi.org/10.1007/s10535-012-0144-9

Mei-zhen ZHANG , L.-n. W., Wei ZHAO , Di GAO , Yu-xian ZHANG , Kui-de YIN. (2023). Effects of salt/alkali-tolerant phosphate-solubilizing bacteria on lipid metabolome of soybean seedlings. *Chinese Journal of Oil Crop Sciences*, *45*(6).

Oi, T., Enomoto, S., Nakao, T., Arai, S., Yamane, K., & Taniguchi, M. (2020). Three-dimensional ultrastructural change of chloroplasts in rice mesophyll cells responding to salt stress. *Annals of Botany*, *125*(5), 833–840. https://doi.org/10.1093/aob/mcz192

Omoto, E. I., Yugo; Miyake, Hiroshi; Taniguchi, Mitsutaka. (2016). Salinity induces membrane structure and lipid changes in maize mesophyll and bundle sheath chloroplasts. *Physiologia Plantarum*, *157*(1), 13–23. https://doi.org/10.1111/ppl.12404

Prasad, R. S. B., P. G.; Hittalmani, S.; Shashidhar, H. E. (2000). Molecular mapping of quantitative trait loci associated with seedling tolerance to salt stress in rice (Oryza sativa L.). *Current Science*, *78*(2), 162–164.

Qi, Y., Guo, X., Li, R., Yin, Y., Wu, X., Wang, J., Li, Y., Zhao, T., Ai, Z., & He, A. (2026). Ion homeostasis coordinates oxidative defense and photosynthesis to sustain rice yield under high-salinity

stress. *Crop and Environment*, *5*(4), 100155. https://doi.org/https://doi.org/10.1016/j.crope.2026.100155

Rachana Ouk, T. O., Daisuke Sugiura, Mitsutaka Taniguchi. (2024). Unravelling the salt stress responses of rice (Oryza sativa L.) mesophyll cells: a three-dimensional analysis. *AoB PLANTS*, *166*(4), plae016. https://doi.org/ 10.1093/aobpla/plae016

Rademacher, W. (2015). Plant Growth Regulators: Backgrounds and Uses in Plant Production. *Journal of Plant Growth Regulation*, *34*(4), 845–872. https://doi.org/10.1007/s00344-015-9541-6

RiceData. (2026). *Monogalactosyldiacylglycerol synthase; MGDG synthase OsMGD1*. https://ricedata.cn/gene/list/47110.htm

Rongjun Zhang, D. Z., Naijie Feng ,Quan-Sheng Qiu ,Hang Zhou,Fengyan Meng ,Xixin Huang ,Anqi Huang ,Yixiang Li. (2023). Prohexadione-calcium alleviates leaf and root damage caused by salt stress in rice (Oryza sativa L.) at the tillering stage. *PLOS ONE*, *18*(2), e0279192. https://doi.org/10.1371/journal.pone.0279192

Sales, C. R. G., Molero, G., Evans, J. R., Taylor, S. H., Joynson, R., Furbank, R. T., Hall, A., Carmo-Silva, E., & Lawson, T. (2022). Phenotypic variation in photosynthetic traits in wheat grown under field versus glasshouse conditions. *Journal of Experimental Botany*, *73*(10), 3221–3237. https://doi.org/10.1093/jxb/erac096

Song, J., Yang, H., Qiao, C., Zhu, C., Bai, T., Du, H., Ma, S., Wang, N., Luo, C., Zhang, Y., Ma, T., Li, P., & Tian, L. (2023). Natural variations of chlorophyll fluorescence and ion transporter genes influenced the differential response of japonica rice germplasm with different salt tolerances [Original Research]. *Frontiers in Plant Science*, *Volume 14 - 2023*. https://doi.org/10.3389/fpls.2023.1095929

Tamanna, N., Mojumder, A., Azim, T., Iqbal, M. I., Alam, M. N. U., Rahman, A., & Seraj, Z. I. (2024). Comparative metabolite profiling of salt sensitive Oryza sativa and the halophytic wild rice Oryza coarctata under salt stress. *Plant-Environment Interactions*, *5*(3), e10155. https://doi.org/https://doi.org/10.1002/pei3.10155

Wang, R., Jing, W., Xiao, L., Jin, Y., Shen, L., & Zhang, W. (2015). The Rice High-Affinity Potassium Transporter1;1 Is Involved in Salt Tolerance and Regulated by an MYB-Type Transcription Factor1[OPEN]. *Plant Physiology*, *168*, 1076 – 1090.

Wang, S., Uddin, M. I., Tanaka, K., Yin, L., Shi, Z., Qi, Y., Mano, J. i., Matsui, K., Shimomura, N., Sakaki, T., Deng, X., & Zhang, S. (2014). Maintenance of Chloroplast Structure and Function by Overexpression of the Rice MONOGALACTOSYLDIACYLGLYCEROL SYNTHASE Gene Leads to Enhanced Salt Tolerance in Tobacco *Plant Physiology*, *165*(3), 1144–1155. https://doi.org/10.1104/pp.114.238899

Welti, R., Li, W., Li, M., Sang, Y., Biesiada, H., Zhou, H.-E., Rajashekar, C. B., Williams, T. D., & Wang, X. (2002). Profiling Membrane Lipids in Plant Stress Responses

ROLE OF PHOSPHOLIPASE Dα IN FREEZING-INDUCED LIPID CHANGES IN ARABIDOPSI. *Journal of Biological Chemistry*, *277*(35), 31994–32002. https://doi.org/10.1074/jbc.M205375200

Xie, W., Liu, H., Ren, D., Wei, Y., Liu, Y., Tang, L., Ding, C., Shao, Z., Qian, Q., & Rao, Y. (2025). A K+-Efflux Antiporter is Vital for Tolerance to Salt Stress in Rice. *Rice*, *18*(1), 57. https://doi.org/10.1186/s12284-025-00815-2

Yadav, S. I., Mohd; Ahmad, Aqil; Hayat, Shamsul. (2011). Causes of salinity and plant manifestations to salt stress: a review. *journal of Environmental Biology*, *32*(5), 667–685.

Yamane, K. K., Michiko; Taniguchi, Mitsutaka; Miyake, Hiroshi. (2008). Correlation between Chloroplast Ultrastructure and Chlorophyll Fluorescence Characteristics in the Leaves of Rice (Oryza sativa L.) Grown under Salinity. *Plant Production Science*, *11*(3), 326–333. https://doi.org/10.1626/pps.11.326

Yang, L., Wang, Y., Bai, Y., Yang, J., Gao, Y., Hou, C., Gao, M., Gu, X., & Liu, W. (2025). Lipid metabolism improves salt tolerance of Salicornia europaea. *Annals of Botany*, *135*(4), 789–802. https://doi.org/10.1093/aob/mcae189

Yang, Y. G., Y. (2018). Elucidating the molecular mechanisms mediating plant salt-stress responses. *New Phytologist*, *217*(2), 523–539. https://doi.org/ 10.1111/nph.14920

Ye, S., Huang, Z., Zhao, G., Zhai, R., Ye, J., Wu, M., Yu, F., Zhu, G., & Zhang, X. (2021). Differential Physiological Responses to Salt Stress between Salt-Sensitive and Salt-Tolerant japonica Rice Cultivars at the Post-Germination and Seedling Stages. *Plants*, *10*(11), 2433.

Yun, P., Shahzad, B., Hasanuzzaman, M., Islam, T., Shabala, L., Zhou, M., Venkataraman, G., Chen, Z.-H., & Shabala, S. (2025). Learning from nature: photosynthetic traits conferring superior salt tolerance in wild rice Oryza coarctata. *Philosophical Transactions of the Royal Society B: Biological Sciences*, *380*(1927). https://doi.org/10.1098/rstb.2024.0242

Zhan, H., Nie, X., Zhang, T., Li, S., Wang, X., Du, X., Tong, W., & Song, W. (2019). Melatonin: A Small Molecule but Important for Salt Stress Tolerance in Plants. *International Journal of Molecular Sciences*, *20*(3), 709.

Zhang, H. I., Louis J.; McGill, Craig; Matthew, Cory; Zhou, Daowei; Kemp, Peter. (2010). The effects of salinity and osmotic stress on barley germination rate: sodium as an osmotic regulator. *Annals of Botany*, *106*(6), 1027–1035. https://doi.org/10.1093/aob/mcq204

Zhang R, Z. D., Feng N, Qiu Q, Zhou H, Liu M, Li Y, Meng F, Huang X, Huang A, Li Y. (2023). Prohexadione calcium enhances rice growth and tillering under NaCl stress. *PeerJ*, *11*, e14804. https://doi.org/10.7717/peerj.14804

Zuo, Z.-F., Li, Y., Mi, X.-F., Li, Y.-L., Zhai, C.-Y., Yang, G.-F., Wang, Z.-Y., & Zhang, K. (2023). Physiological and lipidomic response of exogenous choline chloride alleviating salt stress injury in Kentucky bluegrass (Poa pratensis) [Original Research]. *Frontiers in Plant Science*, *Volume 14 - 2023*. https://doi.org/10.3389/fpls.2023.1269286

Supplementary Files

This is a list of supplementary files associated with this preprint. Click to download.

- file.zip